Gravitational radiation from Kerr black holes using the Sasaki-Nakamura formalism: waveforms and fluxes at infinity

Yucheng Yin,[1, 2, 3, *] Rico K. L. Lo,[1, †] and Xian Chen[2, 3]

[1] *Center of Gravity, Niels Bohr Institute, Blegdamsvej 17, 2100 Copenhagen, Denmark*
[2] *Department of Astronomy, School of Physics, Peking University, 100871 Beijing, China*
[3] *Kavli Institute for Astronomy and Astrophysics at Peking University, 100871 Beijing, China*

(Dated: November 13, 2025)

In linear perturbation theory for Kerr black holes, there are two equivalent formalisms, namely the Teukolsky and the Sasaki-Nakamura (SN) formalism. Typically, one defaults to the Teukolsky formalism, especially when calculating extreme mass ratio inspiral waveforms, and uses the SN formalism when dealing with extended sources, as it offers superior convergence when employing the Green's function method for calculating the inhomogeneous solution. In this work, we present a new scheme for solving the inhomogeneous SN equation, based on integration by parts, that eliminates the extra radial integration step required in the standard formulation to construct the source term for convolution with the SN variable. Our approach enables efficient computations of gravitational waveforms within the SN formalism in *all* cases, from compact to extended sources. We validate our scheme and code implementation against the literature and find excellent agreement, achieving comparable performance without employing any special optimization techniques.

I. INTRODUCTION

It has now been a decade since the first direct detection of a gravitational-wave (GW) signal by the Laser Interferometer Gravitational-Wave Observatory (LIGO) [1] that marks the beginning of GW astronomy. Over the past ten years, we are able to understand much more about astrophysics, such as the population properties of stellar-mass compact binary system [2], fundamental physics, such as black hole (BH) mechanics [3], and more, by analyzing the gravitational waveforms observed by ground-based detectors such as LIGO [4], Virgo [5] and KAGRA [6].

The next big leap in the field of GW astronomy would be the commission of space-based GW detectors such as the Laser Interferometer Space Antenna (LISA) [7]. These space-based detectors target a much lower frequency band—in the millihertz range—compared to those ground-based ones. As a result, they are sensitive to different astrophysical sources of GWs. One such sources is the extreme mass-ratio inspirals (EMRIs) [8], which are the gravitational radiation emitted by massive BHs when perturbed by smaller bodies, such as stars and BHs that are much lighter, orbiting around them.

In contrast to the gravitational waveforms coming from the merger of a stellar-mass compact binary system that we can observe at ground-based detectors effectively infinitely far away, the GW signals coming from EMRIs can remain detectable for months to years instead of just mere seconds [9, 10]. Therefore, it is crucial for us to be able to compute these EMRI waveforms accurately, such that we can compare these theoretical predictions with observations and extract properties about the sources of those EMRIs.

A. Primer in solving for gravitational waveforms from Kerr black holes using Green's functions

The gravitational waveforms that we observe at spatial infinity contain two modes, namely the plus polarization h_+ and the cross polarization $h_\times$, respectively. They are encoded in the perturbed Weyl scalar ψ_4 as [11]

$$\frac{\partial^2}{\partial t^2}\left(h_+ - i h_\times\right) = 2\rho^4 \psi_4, \tag{1}$$

where $\rho = -(r - ia\cos\theta)^{-1}$, and (t, r, θ, φ) are the Boyer-Lindquist (BL) coordinates. In his seminal work, Teukolsky showed that the equation governing the linear perturbation to the scalar ψ_4, which is a partial differential equation, can be solved using separation of variables and a Fourier transform (FT) [12]. Schematically, this decomposition can be written as

$$\psi_4(t, r, \theta, \phi) = \sum_{\ell m \omega} R_{\ell m \omega}(r)\, {}_{-2}S_{\ell m \omega}(\theta, \varphi) e^{-i\omega t}. \tag{2}$$

For the angular sector (θ, φ), the solutions are known as the spin-weighted spheroidal harmonics (SWSHs) ${}_{-2}S_{\ell m \omega}(\theta, \varphi) = {}_{-2}S_{\ell m \omega}(\theta) e^{im\varphi}$. We refer readers to the Appendix A of Ref. [13] for more details. As for the radial sector, the solutions $R_{\ell m \omega}(r)$ are governed by an ordinary differential equation (ODE), aptly referred to as the radial Teukolsky equation in literature, given by

$$\left[\Delta^2 \frac{d}{dr}\left(\frac{1}{\Delta}\frac{d}{dr}\right) - V_{\mathrm{T}}(r)\right] R_{\ell m \omega}(r) = -\mathcal{T}_{\ell m \omega}(r), \tag{3}$$

with a potential V_{T} given by

$$V_{\mathrm{T}}(r) = -\frac{K^2 + 4i(r-1)K}{\Delta} + 8i\omega r + \lambda_{\ell m \omega}, \tag{4}$$

where $\Delta = (r - r_+)(r - r_-)$, $r_\pm = 1 \pm \sqrt{1 - a^2}$, $K = (r^2 + a^2)\omega - ma$, and $\lambda_{\ell m \omega}$ is the separation constant

* yucheng.yin@nbi.ku.dk
† kalok.lo@nbi.ku.dk

from the angular sector. For the sake of simplicity, we will drop the $\ell m\omega$ subscript when there is no risk of confusion hereinafter.

Conceptually, the inhomogeneous radial Teukolsky equation in Eq. (3) can be solved using the Green's function method. We start with two linearly-independent homogeneous solutions that satisfy one of the two boundary conditions for the inhomogeneous solution R^{inhomo} that we want, respectively. In this case, we impose the boundary conditions that the solution is purely ingoing at the horizon and purely outgoing at spatial infinity, and the corresponding homogeneous solutions are denoted by $R^{\mathrm{in}}(r)$ and $R^{\mathrm{up}}(r)$, respectively. Specifically, these solutions have the following asymptotic forms

$$R^{\mathrm{in}}(r) = \begin{cases} B_{\mathrm{T}}^{\mathrm{trans}} \Delta^2 e^{-i\kappa r_*}, & r \to r_+ \\ B_{\mathrm{T}}^{\mathrm{inc}} \dfrac{e^{-i\omega r_*}}{r} + B_{\mathrm{T}}^{\mathrm{ref}} r^3 e^{i\omega r_*}, & r \to \infty \end{cases}, \tag{5}$$

$$R^{\mathrm{up}}(r) = \begin{cases} C_{\mathrm{T}}^{\mathrm{ref}} \Delta^2 e^{-i\kappa r_*} + C_{\mathrm{T}}^{\mathrm{inc}} e^{i\kappa r_*}, & r \to r_+ \\ C_{\mathrm{T}}^{\mathrm{trans}} r^3 e^{i\omega r_*}, & r \to \infty \end{cases}, \tag{6}$$

where $B_{\mathrm{T}}^{\mathrm{trans,inc,ref}}$ and $C_{\mathrm{T}}^{\mathrm{trans,inc,ref}}$ are the transmission, incidence and reflection coefficients for the R^{in} and R^{up} solutions, respectively, and $\kappa = \omega - ma/(2r_+)$.

With these two solutions, we can construct a Green's function $G_{\mathrm{T}}(r, \tilde{r})$ as

$$G_{\mathrm{T}}(r, \tilde{r}) = \begin{cases} \dfrac{1}{W_R} R^{\mathrm{up}}(r) R^{\mathrm{in}}(\tilde{r}), & r > \tilde{r} \\ \dfrac{1}{W_R} R^{\mathrm{in}}(r) R^{\mathrm{up}}(\tilde{r}), & r < \tilde{r} \end{cases}, \tag{7}$$

where W_R is the scaled Wronskian for the two Teukolsky solutions given by

$$W_R = \Delta^{-1} \left(R^{\mathrm{in}} \frac{dR^{\mathrm{up}}}{dr} - R^{\mathrm{up}} \frac{dR^{\mathrm{in}}}{dr} \right). \tag{8}$$

The inhomogeneous solution $R^{\mathrm{inhomo}}(r)$ is then given by

$$\begin{aligned} R^{\mathrm{inhomo}}(r) =& \frac{R^{\mathrm{up}}(r)}{W_R} \int_{r_+}^{r} d\tilde{r} \, \frac{R^{\mathrm{in}}(\tilde{r}) \mathcal{T}(\tilde{r})}{\Delta^2(\tilde{r})} \\ &+ \frac{R^{\mathrm{in}}(r)}{W_R} \int_{r}^{\infty} d\tilde{r} \, \frac{R^{\mathrm{up}}(\tilde{r}) \mathcal{T}(\tilde{r})}{\Delta^2(\tilde{r})} \end{aligned}. \tag{9}$$

As $r \to \infty$, the solution becomes

$$R^{\mathrm{inhomo}}_{\ell m\omega}(r \to \infty) = \underbrace{\frac{1}{2i\omega B_{\mathrm{T}}^{\mathrm{inc}}} \int_{r_+}^{\infty} d\tilde{r} \, \frac{R^{\mathrm{in}}(\tilde{r}) \mathcal{T}(\tilde{r})}{\Delta^2(\tilde{r})}}_{Z^{\infty}_{\ell m\omega}} r^3 e^{i\omega r_*}, \tag{10}$$

where we have substituted an expression for W_R, and we can see that $R^{\mathrm{inhomo}}_{\ell m\omega}$ indeed satisfies the purely outgoing boundary condition at spatial infinity.

Computationally, one will need to first solve the homogeneous radial Teukolsky equation to get $R^{\mathrm{in,up}}(r)$ and the Wronskian W_R before performing the convolution integral over the source term. This can be done using various method, such as the Mano-Suzuki-Takasugi (MST) method [14–16], the Sasaki-Nakamura (SN) formalism [13, 17, 18], and recently a method based on analytical series expansion [19]. When the source term $\mathcal{T}$ is compact (i.e., nonvanishing only at finite values of r), for instance the bound motion of a test particle orbiting around a BH for EMRI waveform modeling, Eq. (10) is perfectly fine for these kind of calculations (see, for example, Ref. [20]).

However, Eq. (10) is no longer suitable for numerical computations when $\mathcal{T}$ is extended and does not decay fast enough. In these cases, the integral for $Z^{\infty}_{\ell m\omega}$ is divergent.[1] A prototypical example of this scenario would be the radial infall of a test particle from infinity towards a BH. In fact, this was the very motivation that led to the development of the SN formalism [17, 18], which gives a well-behaved source term and a convergent convolution integral even when the source is extended.

B. This work

In this paper, we revamp the SN formalism for the driven case to take *full* advantages of the formalism for computing gravitational radiation from Kerr BHs. Specifically, we give a derivation of the source term for the inhomogeneous SN equation that is valid for any equation of motion (i.e., not necessary a geodesic), and introduce a new scheme for solving gravitational waveforms that bypasses the additional integration that was required to obtain the appropriate source term, which is a common criticism of the formalism.

This paper is organized as follows. In Sec. II A, we first review the basics of the SN formalism. Then in Sec. II B, we describe our new scheme for solving the inhomogeneous SN equation using integration by parts, followed by the recipes for computing gravitational waveforms and fluxes at infinity using the SN formalism in Sec. II C. We present in Sec. III A and Sec. III B our results for bound and unbound orbits, respectively. Finally, we discuss some applications, limitations and extensions of this work in Sec. IV.

Throughout this paper, we use geometric units where $c = G = M = 1$. A prime denotes a derivative with respect to r, an overhead dot denotes a derivative with respect to t, while a bar over a variable denotes its complex conjugate. For the normalization conventions of the FT and SWSHs adopted in this paper, refer to Appendix B 1.

II. SASAKI-NAKAMURA FORMALISM

Here we review the basics of the SN formalism for the sake of completeness. In essence, the formalism introduces a new variable $X_{\ell m\omega}$ in place of $R_{\ell m\omega}$ used in the

[1] The Teukolsky formalism itself is still valid. It is just that Eq. (10) is no longer a solution to the inhomogeneous radial Teukolsky equation. See Ref. [21] for a detailed explanation.

Teukolsky formalism. This new variable is constructed such that the ODE it satisfies has a short-ranged potential and a source term that gives a convergent integral when using the Green's function method. We refer readers to Refs. [17, 18] for the detailed construction of the variable.

A. Basics of the Sasaki-Nakamura formalism

The variable $X_{\ell m\omega}$ satisfies the SN equation, which is given by

$$\left[\frac{d^2}{d{r_*}^2} - \mathcal{F}_{\ell m\omega}\frac{d}{dr_*} - \mathcal{U}_{\ell m\omega}\right] X_{\ell m\omega}(r_*) = \mathcal{S}_{\ell m\omega}(r), \quad (11)$$

where

$$\mathcal{F}(r) = \frac{\eta'}{\eta}\frac{\Delta}{r^2+a^2}, \quad (12a)$$

$$\mathcal{U}(r) = \frac{\Delta U_1}{(r^2+a^2)^2} + G^2 + \frac{\Delta G'}{r^2+a^2} - \mathcal{F}G, \quad (12b)$$

$$G(r) = -\frac{2(r-1)}{r^2+a^2} + \frac{r\Delta}{(r^2+a^2)^2}, \quad (12c)$$

$$U_1(r) = V_{\mathrm{T}} + \frac{\Delta^2}{\beta}\left[\left(2\alpha + \frac{\beta'}{\Delta}\right)' - \frac{\eta'}{\eta}\left(\alpha + \frac{\beta'}{\Delta}\right)\right], \quad (12d)$$

with

$$\alpha = 3iK' + \lambda + \frac{6\Delta}{r^2} - i\frac{K\beta}{\Delta^2}, \quad (13a)$$

$$\beta = \Delta\left(-2iK + \Delta' - \frac{4\Delta}{r}\right), \quad (13b)$$

$$\eta = c_0 + \frac{c_1}{r} + \frac{c_2}{r^2} + \frac{c_3}{r^3} + \frac{c_4}{r^4}, \quad (13c)$$

and

$$c_0 = -12i\omega + \lambda(2+\lambda) - 12a\omega\,(a\omega - m)\,, \quad (14a)$$

$$c_1 = 8iam\lambda + 8ia^2\omega(3-\lambda), \quad (14b)$$

$$c_2 = -24ia\,(a\omega - m) + 12a^2\left[1 - 2\,(a\omega - m)^2\right], \quad (14c)$$

$$c_3 = 24ia^3\,(a\omega - m) - 24a^2, \quad (14d)$$

$$c_4 = 12a^4. \quad (14e)$$

Moreover, the ODE is written with respect to the tortoise coordinate r_* given by

$$r_*(r) = \int^r \frac{\tilde{r}^2+a^2}{\Delta}d\tilde{r}, \\ = r + \frac{2r_+}{r_+ - r_-}\ln\frac{r-r_+}{2} - \frac{2r_-}{r_+ - r_-}\ln\frac{r-r_-}{2}. \quad (15)$$

The Teukolsky variable $R_{\ell m\omega}(r)$ in Eq. (3) can be constructed from the SN variable $X_{\ell m\omega}\,(r_*(r))$ in Eq. (11) using

$$R_{\ell m\omega}(r) = \Lambda^{-1}\left[X_{\ell m\omega}(r_*(r))\right] + \frac{\left(r^2+a^2\right)^{3/2}}{\eta}\mathcal{S}_{\ell m\omega}, \quad (16)$$

where Λ^{-1} is the differential operator for the inverse SN transformation defined as

$$\Lambda^{-1}\left[X_{\ell m\omega}\right] = \frac{1}{\eta}\left[\frac{\alpha\Delta + \beta'}{\sqrt{r^2+a^2}}X_{\ell m\omega} - \frac{\beta}{\Delta}\left(\frac{\Delta X_{\ell m\omega}}{\sqrt{r^2+a^2}}\right)'\right]. \quad (17)$$

Comparing Eq. (16) with the homogeneous case, e.g., in Ref. [13], we see that there is now an additional contribution coming from the source term $\mathcal{S}_{\ell m\omega}$. By construction, $\mathcal{S}_{\ell m\omega}$ decays fast enough as $r\to\infty$ such that it does not contribute to Eq. (16). Importantly, this implies that

$$R_{\ell m\omega}(r\to\infty) = \lim_{r\to\infty}\Lambda^{-1}\left[X_{\ell m\omega}(r_*(r))\right]. \quad (18)$$

The derivation of the expression relating the SN source term $\mathcal{S}_{\ell m\omega}$ with the Teukolsky source term $\mathcal{T}_{\ell m\omega}$ can be found in Appendix A. Here, we just state the result, which is

$$\mathcal{S}_{\ell m\omega} = \frac{\eta\Delta\mathcal{W}}{(r^2+a^2)^{3/2}r^2}\exp\left(-i\int^r\frac{K}{\Delta}d\tilde{r}\right), \quad (19)$$

where we define an auxiliary function $\mathcal{W}(r)$ related to the Teukolsky source term $\mathcal{T}_{\ell m\omega}$ by

$$\frac{d^2\mathcal{W}}{dr^2} = -\frac{r^2}{\Delta^2}\mathcal{T}_{\ell m\omega}(r)\exp\left(i\int^r\frac{K}{\Delta}d\tilde{r}\right). \quad (20)$$

The Teukolsky source term $\mathcal{T}_{\ell m\omega}$ itself for a point particle is given by [22]

$$\mathcal{T}_{\ell m\omega}(r) = \mu\int_\gamma d\tau\; e^{i\omega t(\tau) - im\varphi(\tau)} \\ \Delta^2\left\{\left(A_{nn0} + A_{n\bar{m}0} + A_{\bar{m}\bar{m}0}\right)\delta(r - r(\tau)) \right. \\ + \left[\left(A_{n\bar{m}1} + A_{\bar{m}\bar{m}1}\right)\delta(r - r(\tau))\right]' \\ \left. + \left[A_{\bar{m}\bar{m}2}\delta(r - r(\tau))\right]''\right\}, \quad (21)$$

where μ is the mass of the particle and γ denotes its trajectory. The expressions of A_{nn0}, $A_{n\bar{m}0}$, $A_{\bar{m}\bar{m}0}$, $A_{n\bar{m}1}$, $A_{\bar{m}\bar{m}1}$, $A_{\bar{m}\bar{m}1}$ can be found in Appendix B.

We can solve the inhomogeneous SN equation using the Green's function method. Similarly, we need X^{in} and X^{up} that satisfy the purely ingoing boundary condition at the horizon and purely outgoing boundary condition at spatial infinity, respectively. Asymptotically, they are given by

$$X^{\mathrm{in}}(r_*) = \begin{cases} B^{\mathrm{trans}}_{\mathrm{SN}}e^{-i\kappa r_*} & r_*\to-\infty \\ B^{\mathrm{inc}}_{\mathrm{SN}}e^{-i\omega r_*} + B^{\mathrm{ref}}_{\mathrm{SN}}e^{i\omega r_*} & r_*\to\infty \end{cases}, \quad (22)$$

and

$$X^{\mathrm{up}}(r_*) = \begin{cases} C^{\mathrm{ref}}_{\mathrm{SN}}e^{-i\kappa r_*} + C^{\mathrm{inc}}_{\mathrm{SN}}e^{i\kappa r_*} & r_*\to-\infty \\ C^{\mathrm{trans}}_{\mathrm{SN}}e^{i\omega r_*} & r_*\to\infty \end{cases}, \quad (23)$$

where $B_{\rm SN}^{\rm trans,inc,ref}$ and $C_{\rm SN}^{\rm trans,inc,ref}$ are the transmission, incidence and reflection coefficients for the $X^{\rm in}$ and $X^{\rm up}$ solutions, respectively. The inhomogeneous solution $X^{\rm inhomo}(r_*)$ is then given by

$$\begin{aligned} X_{\ell m\omega}^{\rm inhomo}(r_*) =& \frac{X_{\ell m\omega}^{\rm up}(r_*)}{W_X}\int_{-\infty}^{r_*} X_{\ell m\omega}^{\rm in}(\tilde{r}_*)\frac{\mathcal{S}_{\ell m\omega}(\tilde{r}_*)}{\eta}d\tilde{r}_* \\ &+ \frac{X_{\ell m\omega}^{\rm in}(r_*)}{W_X}\int_{r_*}^{\infty} X_{\ell m\omega}^{\rm up}(\tilde{r}_*)\frac{\mathcal{S}_{\ell m\omega}(\tilde{r}_*)}{\eta}d\tilde{r}_*, \end{aligned} \tag{24}$$

where W_X is the scaled Wronskian[2] defined by

$$W_X = \frac{1}{\eta}\left[X_{\ell m\omega}^{\rm in}\frac{dX_{\ell m\omega}^{\rm up}}{dr_*} - X_{\ell m\omega}^{\rm up}\frac{dX_{\ell m\omega}^{\rm in}}{dr_*}\right] = \frac{2i\omega}{c_0}B_{\rm SN}^{\rm inc}C_{\rm SN}^{\rm trans}. \tag{25}$$

In particular, when $r_* \to \infty$, the inhomogeneous SN solution becomes

$$X_{\ell m\omega}^{\rm inhomo}(r_* \to \infty) = \underbrace{\frac{c_0}{2i\omega B_{\rm SN}^{\rm inc}}\int_{-\infty}^{\infty}\frac{X_{\ell m\omega}^{\rm in}(r_*)\mathcal{S}_{\ell m\omega}(r_*)}{\eta}dr_*}_{X_{\ell m\omega}^{\infty}}\, e^{i\omega r_*}. \tag{26}$$

Using Eq. (18), one can relate the asymptotic amplitude at infinity $X_{\ell m\omega}^{\infty}$ with $Z_{\ell m\omega}^{\infty}$, which means

$$R_{\ell m\omega}^{\rm inhomo} = -\frac{4\omega^2}{c_0}X_{\ell m\omega}^{\infty}r^3e^{i\omega r_*}. \tag{27}$$

The GW polarizations h_+ and $h_\times$ can then be expressed as

$$h_+ - ih_\times = -\frac{2}{r}\sum_{\ell m}\int_{-\infty}^{\infty}\frac{Z_{\ell m\omega}^{\infty}}{\omega^2}{}_{-2}S_{\ell m\omega}(\theta)e^{-i\omega(t-r_*)+im\varphi}d\omega, \tag{28}$$

where

$$Z_{\ell m\omega}^{\infty} = -\frac{4\omega^2}{c_0}X_{\ell m\omega}^{\infty}. \tag{29}$$

B. New scheme for solving the inhomogeneous Sasaki-Nakamura equation using integration by parts

Conventionally, solving for gravitational waveforms $h_{+,\times}$ using the SN formalism requires first integrating Eq. (20) for $\mathcal{W}$ [and hence $\mathcal{S}$ through Eq. (19)], often numerically, and then integrating the convolution integral of some homogeneous solution X with the source term $\mathcal{S}$ in Eq. (26) for $X_{\ell m\omega}^{\infty}$. Comparing with Eq. (10), where the source term $\mathcal{T}$ in the convolution integral often has an analytical expression, the SN formalism seems to be at a disadvantage. However, this does *not* have to be the case. Here, we show that by using integration by parts (IBP) twice with the help of an auxiliary function, one can convert the convolution integral in the SN formalism to use the Teukolsky source term $\mathcal{T}$.

We first define two auxiliary functions $Y_{\ell m\omega}^{\rm in/up}(r)$, respectively, where

$$Y_{\ell m\omega}^{\rm in/up\,\prime\prime}(r) \equiv \frac{X_{\ell m\omega}^{\rm in/up}(r)}{r^2\sqrt{r^2+a^2}}\exp\left(-i\int^r\frac{K}{\Delta}dr\right). \tag{30}$$

Furthermore, we replace $X_{\ell m\omega}^{\rm in/up}$ with $Y_{\ell m\omega}^{\rm in/up}$ in Eq. (24), we can obtain

$$\begin{aligned} X_{\ell m\omega}^{\rm inhomo}(r_*) =& \frac{X_{\ell m\omega}^{\rm up}(r_*)}{W_X}\int_{r_+}^{r(r_*)} Y_{\ell m\omega}^{\rm in\,\prime\prime}\mathcal{W}(r)dr \\ &+ \frac{X_{\ell m\omega}^{\rm in}(r_*)}{W_X}\int_{r(r_*)}^{\infty} Y_{\ell m\omega}^{\rm up\,\prime\prime}\mathcal{W}(r)dr. \end{aligned} \tag{31}$$

Now Eq. (24) is rewritten in a suggestive form. We can apply IBP twice to swap the differentiation (with respect to r) from Y to $\mathcal{W}$, at the expense of picking up extra boundary terms where

$$\begin{aligned} X_{\ell m\omega}^{\rm inhomo}(r_*) =& \frac{X_{\ell m\omega}^{\rm up}(r_*)}{W_X}\int_{r_+}^{r(r_*)} Y_{\ell m\omega}^{\rm in}\frac{d^2\mathcal{W}(r)}{dr^2}dr \\ &+ \frac{X_{\ell m\omega}^{\rm up}(r_*)}{W_X}\left[Y_{\ell m\omega}^{\rm in\,\prime}(r)\mathcal{W}(r) - Y_{\ell m\omega}^{\rm in}(r)\mathcal{W}'(r)\right]_{r_+}^{r(r_*)} \\ &+ \frac{X_{\ell m\omega}^{\rm in}(r_*)}{W_X}\left[Y_{\ell m\omega}^{\rm up\,\prime}(r)\mathcal{W}(r) - Y_{\ell m\omega}^{\rm up}(r)\mathcal{W}'(r)\right]_{r(r_*)}^{\infty} \\ &+ \frac{X_{\ell m\omega}^{\rm in}(r_*)}{W_X}\int_{r(r_*)}^{\infty} Y_{\ell m\omega}^{\rm up}\frac{d^2\mathcal{W}(r)}{dr^2}dr. \end{aligned} \tag{32}$$

Specifically, we are interested in the case when $r_* \to \infty$, i.e.,

$$\begin{aligned} X_{\ell m\omega}^{\infty} =& \frac{c_0}{2i\omega B_{\rm SN}^{\rm inc}}\left[Y_{\ell m\omega}^{\rm in\,\prime}(r)\mathcal{W}(r) - Y_{\ell m\omega}^{\rm in}(r)\mathcal{W}'(r)\right]_{r_+}^{\infty} \\ &+ \frac{c_0}{2i\omega B_{\rm SN}^{\rm inc}}\int_{r_+}^{\infty} Y_{\ell m\omega}^{\rm in}(r)\frac{d^2\mathcal{W}(r)}{dr^2}dr. \end{aligned} \tag{33}$$

This is the key result of the paper — if we can discard the boundary terms (which later in the text we show that this is justified in some cases), then we can calculate $X_{\ell m\omega}^{\infty}$ without having to solve for $\mathcal{W}$. Additionally, the new auxiliary function $Y_{\ell m\omega}^{\rm in}$ introduced here does *not* depend on the source term and can be constructed easily from the homogeneous solution $X_{\ell m\omega}^{\rm in}$, which will be the subject of Sec. II B 1.

By inserting Eq. (20) into Eq. (33), the convolution integral in our new scheme can be written as

$$
\begin{aligned}
I &= \int_{r_+}^{\infty} Y^{\rm in}(r)\frac{d^2\mathcal{W}(r)}{dr^2}dr \\
&= -\int_{r_+}^{\infty} Y^{\rm in}(r)\frac{r^2}{\Delta^2}\mathcal{T}_{\ell m\omega}(r)\exp\left(i\int^r \frac{K}{\Delta}d\tilde{r}\right)dr \\
&= -\mu\int_{r_+}^{\infty}\int_{\gamma} r^2 Y^{\rm in}(r)\exp\left(i\int^r \frac{K}{\Delta}d\tilde{r}\right)\Big[\left(A_{nn0}+A_{\bar{m}n0}+A_{\bar{m}\bar{m}0}\right)\delta(r-r(\tau)) \\
&\qquad + \left\{\left(A_{\bar{m}n1}+A_{\bar{m}\bar{m}1}\right)\delta(r-r(\tau))\right\}_{,r} + \left\{A_{\bar{m}\bar{m}2}\delta(r-r(\tau))\right\}_{,rr}\Big]e^{i\omega t(\tau)-im\varphi(\tau)}d\tau dr \\
&= -\mu\int_{\gamma}\Big[\mathcal{Y}(r)\left(A_{nn0}+A_{\bar{m}n0}+A_{\bar{m}\bar{m}0}\right)-\mathcal{Y}'(r)\left(A_{\bar{m}n1}+A_{\bar{m}\bar{m}1}\right) \\
&\qquad\qquad + \mathcal{Y}''(r)A_{\bar{m}\bar{m}2}\Big]_{r=r(\tau),\theta=\theta(\tau)}e^{i\omega t(\tau)-im\varphi(\tau)}d\tau,
\end{aligned}
\tag{34}
$$

where we define for convenience

$$
\mathcal{Y}(r) = r^2 Y^{\rm in}(r)\exp\left(i\int^r \frac{K}{\Delta}d\tilde{r}\right). \tag{35}
$$

Notice that we have exchanged the order of the $d\tau$ integral and the dr integral in the last equality of Eq. (34). This allows us to eliminate the Dirac delta function and its derivative and evaluate the integral along the particle trajectory.

In fact, by simplifying the expression enclosed in the square brackets in the last equality of Eq. (34), we can obtain a very elegant expression for I as

$$
I = -\mu\int_{\gamma}\left[\mathcal{N}^2(\tau)W_{nn}(\tau)+\mathcal{N}(\tau)\bar{\mathcal{M}}(\tau)W_{n\bar{m}}(\tau)+\bar{\mathcal{M}}^2(\tau)W_{\bar{m}\bar{m}}(\tau)\right]e^{i\omega t(\tau)-im\varphi(\tau)}d\tau, \tag{36}
$$

where

$$
\mathcal{N} = u^t - a\sin^2\theta u^{\varphi} + \frac{\Sigma}{\Delta}u^r, \tag{37a}
$$

$$
\bar{\mathcal{M}} = ia\sin\theta u^t - i\left(r^2+a^2\right)\sin\theta u^{\varphi} + \Sigma u^{\theta}, \tag{37b}
$$

with u denoting the four velocity of the particle and $\Sigma = r^2 + a^2\cos^2\theta$. Note that Eq. (36) holds also for non-geodesic motions. The W terms (not to be confused with $\mathcal{W}$) represent the coupling between the auxiliary function $Y(r)$ and certain structures of the source, while $\mathcal{N}$ and $\bar{\mathcal{M}}$ contain the information about the motion of the particle along the n_μ and $\bar{m}_\mu$ direction in the Newman-Penrose tetrad, respectively. The expressions for the W terms can be found in Appendix B.

1. *The $Y(r)$ function*

A core ingredient of our new SN-IBP approach is the auxiliary functions $Y^{\rm in,up}$, which are constructed as the solutions to the second order ODE in Eq. (30) subjecting to different initial conditions, respectively. Here, we give a prescription on how to solve for these functions.

For the $Y^{\rm in}$ function, we impose the initial conditions that $Y^{\rm in}(r\to\infty) = Y^{\rm in\prime}(r\to\infty) = 0$. Unfortunately, Eq. (30) needs to be integrated numerically. To speed up the computation, we expand $Y^{\rm in\prime\prime}$ near infinity as

$$
Y^{\rm in\prime\prime}(r\to\infty) = \frac{B^{\rm ref}_{\rm SN}}{r^3}\sum_{j=0}^{\infty}\frac{Y^{\infty}_{+,j}}{r^j} + \frac{B^{\rm inc}_{\rm SN}e^{4i\omega\ln 2-2i\omega r}}{r^{3+4i\omega}}\sum_{j=0}^{\infty}\frac{Y^{\infty}_{-,j}}{r^j}, \tag{38}
$$

where the coefficients $Y^{\infty}_{\pm,j}$ are given in Appendix C 1. This allows us to start the numerical integration for $Y^{\rm in}$ at a smaller outer boundary since we can analytically integrate Eq. (38) to evaluate the proper initial values to use at the outer boundary.

In addition, we found that it is easier to integrate the ODE in r_* instead, which is now given by

$$
\frac{d^2Y}{dr_*^2} = \frac{2(r^2-a^2)}{(r^2+a^2)^2}\frac{dY}{dr_*} + \frac{\Delta^2 X(r_*)}{r^2(r^2+a^2)^{5/2}}\exp\left(-i\int^r\frac{K}{\Delta}d\tilde{r}\right), \tag{39}
$$

where we have omitted the $\{\rm in, up\}$ superscript for sim-

[2] The scaled Wronskain defined for the SN variable X is in fact identical to that defined for the Teukolsky variable R. Refer to Appendix E of Ref. [13] for a proof.

plicity.[3] As an example, Fig. 1 shows the solution for $Y^{\rm in}(r_*)$ and $Y^{\rm in\prime}(r_*)$ with $\ell = m = 2$, $a/M = 0.9$, and $M\omega = 1$, 0.5, and 0.1. We see that both $Y(r_* \to \infty)$ and $Y'(r_* \to \infty)$ converge to zero, while $Y(r_* \to -\infty)$ and $Y'(r_* \to -\infty)$ are constants. Importantly, Y and Y' are nonoscillatory at both ends, unlike the Teukolsky variable R or the SN variable X.

Similarly, for the $Y^{\rm up}$ function, we impose the initial conditions that $Y^{\rm up}(r = r_+) = Y^{\rm up\prime}(r = r_+) = 0$. We expand $Y^{\rm up\prime\prime}$ near the horizon as

$$Y^{\rm up\prime\prime}(r \to r_+) = C^{\rm inc}_{\rm SN} \sum_{j=0}^{\infty} Y^{\rm H}_{+,j}\,(r - r_+)^j + C^{\rm ref}_{\rm SN}\,(r - r_+)^{i\frac{(ar_+ m + 2a^2\omega - 4r_+\omega)}{r_+\sqrt{1-a^2}}} \sum_{j=0}^{\infty} Y^{\rm H}_{+,j}\,(r - r_+)^j\,, \tag{40}$$

where the coefficients $Y^{\rm H}_{\pm,j}$ are given in Appendix C 2. Again, this allows us to start the numerical integration for $Y^{\rm up}$ at a finite inner boundary (in r_*) since we can analytically integrate Eq. (40) to obtain the proper initial values to use at the inner boundary.

2. *The $\mathcal{W}(r)$ function*

Another ingredient that is needed for the SN formalism is the $\mathcal{W}$ function, which in turns gives the actual source term for the inhomogeneous SN equation. While we refer readers to Appendix A of Ref. [23] where the general solution of $\mathcal{W}(r)$ for a generic geodesic was presented, here we re-derive these formulas using notations consistent with this paper for the sake of clarity.

The key to deriving the expression for $\mathcal{W}(r)$ lies in decoupling the terms related to $\mathcal{N}$ and $\bar{\mathcal{M}}$, respectively, and decomposing the expression using IBP. This improves the convergence of the integrand. Meanwhile, the expressions outside the integral reflect the asymptotic behavior of $\mathcal{W}(r)$ at infinity. Integrating the resultant expression inward from infinity then yields the final expression of $\mathcal{W}(r)$.

In addition, we also need to use two crucial identities. One is associated with $\mathcal{N}$ and the other with $\bar{\mathcal{M}}$. In Ref. [23], these derivations and identities are restricted to geodesic motions. Here, we show that these identities and expressions remain valid in all cases including nongeodesics.

When solving for $\mathcal{W}(r)$ in Eq. (20) [not to be confused with W defined in Eq. (36)], we generally partition it into three terms, namely

$$\mathcal{W}(r) = \mathcal{W}_{nn}(r) + \mathcal{W}_{n\bar{m}}(r) + \mathcal{W}_{\bar{m}\bar{m}}(r). \tag{41}$$

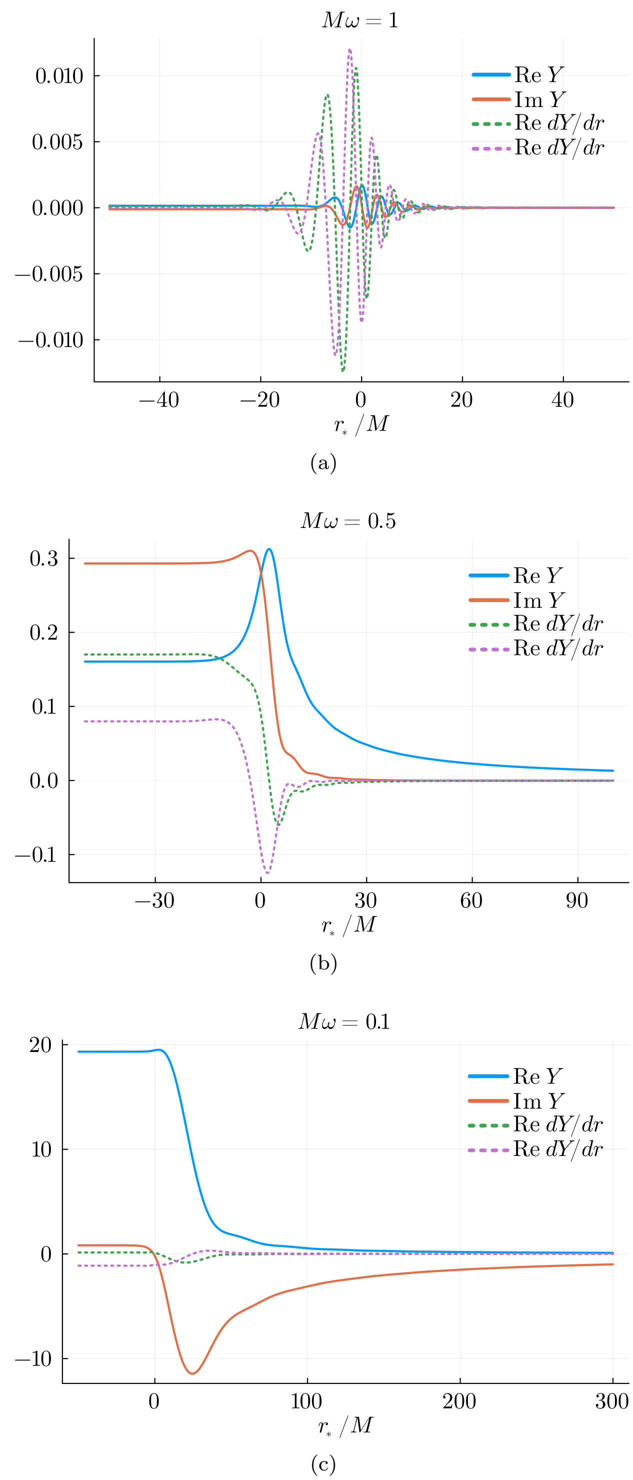

FIG. 1. The $Y^{\rm in}$ solutions for Eq. (30) with boundary conditions $Y^{\rm in}(r \to \infty) = Y^{\rm in\prime}(r \to \infty) = 0$ and $\ell = m = 2$, $a/M = 0.9$. From the top to the bottom, the frequency is set to $M\omega = 1$, 0.5, and 0.1, respectively.

[3] Notice that the term $\exp\left(\pm i \int^r \frac{K}{\Delta} d\tilde{r}\right)$ can be evaluated analytically [cf Eq. (B2d)].

In particular, we use $\mathcal{W}_{nn}$ as an example to present part of the derivation. This is because $\mathcal{W}_{nn}$ will be used in our subsequent analysis of GWs excited by particles falling radially along the spin axis (see Sec. III B). The results for $\mathcal{W}_{n\bar{m}}$ and $\mathcal{W}_{\bar{m}\bar{m}}$ will be given without detailed derivation.

It is not difficult to show from Eq. (20) and Eq. (21) that $\mathcal{W}_{nn}$ satisfies the ODE

$$\begin{aligned}\frac{d^2\mathcal{W}_{nn}}{dr^2}=&-\frac{\mathscr{A}\mu}{2}r^2\exp\left(i\int^r\frac{K}{\Delta}d\tilde{r}\right)\int_\gamma d\tau\ e^{i\omega t(\tau)-im\varphi(\tau)}\rho\bar{\rho}^2\mathcal{N}^2\mathscr{L}_1^\dagger\left[\rho^{-4}\mathscr{L}_2^\dagger\left(\rho^3S\right)\right]\delta(r-r(\tau))\\ =&-\frac{\mathscr{A}\mu}{2}\sum_j\left\{\frac{1}{u^r}r^2\rho\bar{\rho}^2\mathcal{N}^2\mathscr{L}_1^\dagger\left[\rho^{-4}\mathscr{L}_2^\dagger\left(\rho^3S\right)\right]e^{i\chi(r)}\right\}_{r=r(\tau_j)},\end{aligned}\tag{42}$$

where $\mathscr{L}_s^\dagger\equiv\partial_\theta-m/\sin\theta+a\omega\sin\theta+s\cot\theta$ is a differential operator on the angular sector and

$$\chi(r)\equiv\omega t(r)-m\varphi(r)+\int^r\frac{K}{\Delta}d\tilde{r}=\omega v(r)-m\tilde{\varphi}(r),\tag{43}$$

with $v=t+r_*$ and $\tilde{\varphi}=\varphi+\int^r\frac{a}{\Delta}d\tilde{r}$ defined as Kerr ingoing coordinates. Note that Eq. (42) is a more general version of Eq. (A25) in Ref. [23], where there was no $\sum_j^{r=r_j}$ summation in the expression. The summation here is defined such that the particle is located at r when $\tau=\tau_1,\tau_2,\cdots,\tau_j$. For unidirectional trajectories, e.g., radial infalls and quasicircular plunges, we have $j=1$ and the summation can be omitted. While for bound orbits, $j=\infty$, and for scattering orbits, $j=2$. Most of the previous works have considered the case when $j=1$ only, i.e., a particle moves unidirectionally.

For cases where $j>1$, we should divide the orbit into multi-unidirectional pieces. Divisions are at the turning points where $u^r=0$. At these turning points, the denominator becomes zero, making the expression singular. However, this does not affect the subsequent integrations, as these singular points of the integrand can be transformed into a smooth form through changing the integration variable. For details, see Ref. [24] for scattering orbits and Ref. [25] for spherical-inclined bound orbits.

Here, we first suppose that the trajectory is unidirectional and omit the summation. By taking the r-derivative of $\chi(r)$, one can show that

$$\chi'(r)=\omega\frac{\mathcal{N}}{u^r}+\left(a\omega\sin^2\theta-m\right)\tilde{\varphi}'.\tag{44}$$

Therefore, we can obtain an identity related to $\mathcal{N}$ that reads

$$\begin{aligned}f(r)\frac{\mathcal{N}}{u^r}e^{i\chi(r)}=&\frac{1}{i\omega}\left\{\left[f(r)e^{i\chi(r)}\right]'\right.\\&\left.-\left[f'(r)+i\xi(r)f(r)\right]e^{i\chi(r)}\right\},\end{aligned}\tag{45}$$

where

$$\xi(r)=\left(a\omega\sin^2\theta-m\right)\tilde{\varphi}'(r)\sim\mathcal{O}\left(r^{-3/2}\right),\tag{46}$$

and $f(r)$ is an arbitrary smooth function of r. By integrating Eq. (42) and using Eq. (45) twice, we obtain the expression of $\mathcal{W}_{nn}$ as a three-term form. Similarly, one can obtain the expressions of $\mathcal{W}_{n\bar{m}}$ and $\mathcal{W}_{\bar{m}\bar{m}}$ with the help of the identity in Eq. (A7). Schematically, they are

$$\frac{1}{\mu}\mathcal{W}_{nn}(r)=f_0(r)e^{i\chi(r)}+\int_r^\infty f_1(r_1)e^{i\chi(r_1)}dr_1+\int_r^\infty dr_1\int_{r_1}^\infty f_2(r_2)e^{i\chi(r_2)}dr_2,\tag{47a}$$

$$\frac{1}{\mu}\mathcal{W}_{n\bar{m}}(r)=g_0(r)e^{i\chi(r)}+\int_r^\infty g_1(r_1)e^{i\chi(r_1)}dr_1+\int_r^\infty dr_1\int_{r_1}^\infty g_2(r_2)\ e^{i\chi(r_2)}dr_2,\tag{47b}$$

$$\frac{1}{\mu}\mathcal{W}_{\bar{m}\bar{m}}(r)=h_0(r)e^{i\chi(r)}+\int_r^\infty h_1(r_1)e^{i\chi(r_1)}dr_1+\int_r^\infty dr_1\int_{r_1}^\infty h_2(r_2)\ e^{i\chi(r_2)}dr_2,\tag{47c}$$

where the expressions of $f_{0,1,2}$, $g_{0,1,2}$, and $h_{0,1,2}$ can be found in Appendix D.

Moreover, for bound orbits, Eq. (20) actually reads

$$\begin{aligned}\mathcal{W}''=&-\frac{r^2}{\Delta^2}\mathcal{T}\exp\left(i\int^r\frac{K}{\Delta}d\tilde{r}\right)\\&\times\Theta(r-r_{\rm min})\Theta(r_{\rm max}-r),\end{aligned}\tag{48}$$

where $\Theta(x)$ is the Heaviside step function, $r_{\rm min}$ and $r_{\rm max}$ are the inner and outer edges of the orbit. Thus, we need to multiply all of the f, g and h functions in Eqs. (47) by $\Theta(r-r_{\rm min})\Theta(r_{\rm max}-r)$. This implies that

$$\mathcal{W}(r)=\mathcal{W}'(r)=0 \qquad r>r_{\rm max}. \tag{49}$$

In Sec. II C 1, we will see that this result allows us to discard boundary terms when using the SN-IBP method.

3. The boundary terms $Y'\mathcal{W}$ and $Y\mathcal{W}'$

Recall from Eq. (32) that for our SN-IBP approach, we need to evaluate $Y'(r)\mathcal{W}(r)$ and $Y(r)\mathcal{W}'(r)$ at both the horizon and infinity, respectively. Here, we will discuss when it is justified to discard these boundary terms.

The general solutions of $Y(r)$ and $\mathcal{W}(r)$ can be written as

$$\begin{aligned} Y(r) &= Y^{\rm part}(r)+y_1 r+y_0,\\ \mathcal{W}(r) &= \mathcal{W}^{\rm part}(r)+w_1 r+w_0, \end{aligned} \tag{50}$$

where $Y^{\rm part}$ and $\mathcal{W}^{\rm part}$ are the particular solutions to Eq. (30) and Eq. (20) that we gave earlier in the paper, respectively, and $y_{0,1}$, $w_{0,1}$ are some constants. We can choose these constants to our advantages. Moreover, we will refer to the particular solution of $Y(r)$ obtained in Sec. II B 1 [$Y^{\rm part}(r\to\infty)=Y^{\rm part\prime}(r\to\infty)=0$] with $y_0=y_1=0$ as the canonical solution of Eq. (30), and similarly we will refer to the particular solution of $\mathcal{W}(r)$ obtained in Sec. II B 2 with $w_0=w_1=0$ as the canonical solution of Eq. (20).

In general, the canonical solution $\mathcal{W}^{\rm canonical}(r)$ has the asymptotic behaviors

$$\mathcal{W}^{\rm canonical}(r)\sim\begin{cases}\mathcal{O}(1), & r\to r_+\\ \mathcal{O}(r^{1/2}), & r\to\infty\end{cases}, \tag{51}$$

and

$$\mathcal{W}^{\rm canonical\prime}(r)\sim\begin{cases}\mathcal{O}(1), & r\to r_+\\ \mathcal{O}(1), & r\to\infty\end{cases}. \tag{52}$$

If one chooses the canonical solution as the particular solution and set

$$w_0=-\mathcal{W}^{\rm part}(r_+)+r_+\mathcal{W}^{\rm part\prime}(r_+), \tag{53a}$$
$$w_1=-\mathcal{W}^{\rm part\prime}(r_+), \tag{53b}$$

then the boundary terms of $\mathcal{W}(r)$ at the horizon vanish [26]. However, this assumes that the limits $\mathcal{W}^{\rm part}(r\to r_+)$ and $\mathcal{W}^{\rm part\prime}(r\to r_+)$ exist. From the analysis in Sec. II B 2, this requirement translates into the condition that the limit $\chi(r\to r_+)$ exists.

When a particle is close enough to the horizon of a BH, all external forces will be negligible compared to the influence of spacetime curvature itself. This means that the particle moves along a geodesic when approaching the horizon. Therefore, we can use the geodesic equations and obtain

$$\frac{d\chi}{dr_*}\sim\mathcal{O}(\Delta), \qquad r_*\to-\infty. \tag{54}$$

As a result, we have

$$\chi(r_*\to-\infty)=\text{const.} \tag{55}$$

With this choice of $w_{0,1}$, we have the following asymptotic behaviors for $\mathcal{W}$ as

$$\mathcal{W}(r)\sim\begin{cases}\mathcal{O}(\Delta^2), & r\to r_+\\ \mathcal{O}(r), & r\to\infty\end{cases}, \tag{56}$$

and

$$\mathcal{W}'(r)\sim\begin{cases}\mathcal{O}(\Delta), & r\to r_+\\ \mathcal{O}(1), & r\to\infty\end{cases}, \tag{57}$$

at the expense that $\mathcal{W}(r\to\infty)$ becomes less convergent.[4]

Similarly, the canonical solution $Y^{\rm canonical}(r)$ has the asymptotic behaviors (which can also be seen in Fig. 1) as

$$Y^{\rm canonical}(r)\sim\begin{cases}\mathcal{O}(1), & r\to r_+\\ \mathcal{O}(1/r), & r\to\infty\end{cases}, \tag{58}$$

and

$$Y^{\rm canonical\prime}(r)\sim\begin{cases}\mathcal{O}(1), & r\to r_+\\ \mathcal{O}(1/r^2), & r\to\infty\end{cases}. \tag{59}$$

By setting

$$y_0=-Y^{\rm part}(r_+)+r_+Y^{\rm part\prime}(r_+), \tag{60a}$$
$$y_1=-Y^{\rm part\prime}(r_+), \tag{60b}$$

we can obtain a solution with the asymptotic behaviors where

$$Y(r)\sim\begin{cases}\mathcal{O}(\Delta^2), & r\to r_+\\ \mathcal{O}(r), & r\to\infty\end{cases}, \tag{61}$$

and

$$Y'(r)\sim\begin{cases}\mathcal{O}(\Delta), & r\to r_+\\ \mathcal{O}(1), & r\to\infty\end{cases}. \tag{62}$$

In the next subsection, we give the recipes to calculate gravitational waveforms and fluxes at infinity using the SN formalism with these ingredients.

[4] Note that $\mathcal{S}$ is still convergent when $r\to\infty$.

C. Recipes for calculating waveforms and fluxes at infinity

1. Bound orbits

We have seen from Eq. (49) that the canonical solution of $\mathcal{W}(r)$ for bound orbits, i.e., $w_0 = w_1 = 0$, vanishes at infinity. Therefore, we only need to:

1. Solve for $Y(r)$ following the scheme introduced in Sec. II B 1.
2. Extract the boundary values of $Y(r)$ and $Y'(r)$ at the horizon and calculate y_0 and y_1 following Eqs. (60).

With these choices, all four of the boundary terms in Eq. (33) vanish. We can then calculate the inhomogeneous solution using Eq. (36), and therefore the gravitational waveform and fluxes at infinity.

Here, we briefly introduce a procedure for calculating the amplitude for each harmonic of an EMRI waveform on a generic bound geodesic. The derivation is analogous to the one in Ref. [20], but under the SN formalism. Then, in Sec. III A, we show some examples of EMRIs waveforms on generic (eccentric-inclined) orbits using our SN-IBP scheme.

A generic bound geodesic orbit in the BL coordinates can be decoupled into harmonics of r and θ. This is because the Kerr metric components have no dependence on t and φ. The general solutions to the timelike bound geodesic equation can be expressed as

$$t(\lambda) = \Gamma\lambda + \Delta t[r(\lambda), \theta(\lambda)], \tag{63a}$$

$$r(\lambda) = \sum_{n=-\infty}^{\infty} r_n e^{-in\Upsilon_r\lambda}, \tag{63b}$$

$$\theta(\lambda) = \sum_{k=-\infty}^{\infty} \theta_k e^{-ik\Upsilon_\theta\lambda}, \tag{63c}$$

$$\varphi(\lambda) = \Upsilon_\varphi\lambda + \Delta\varphi[r(\lambda), \theta(\lambda)], \tag{63d}$$

where Γ, Υ_r, Υ_θ, Υ_φ are frequencies parametrized by the Mino time λ which is defined by $d\tau = \Sigma d\lambda$. To help with our calculations, we also introduce an open source `julia` package `KerrGeodesics.jl` for solving timelike Kerr geodesics, see Appendix E for details.

Therefore, we can write the Green's function integral Eq. (36) as

$$I = -\mu \int_\gamma J_{\ell m\omega}\left[r(\lambda), \theta(\lambda)\right] e^{i(\omega\Gamma - m\Upsilon_\varphi)\lambda} d\lambda. \tag{64}$$

The integrand kernel is defined by

$$\begin{aligned} J_{\ell m\omega} &= \frac{d\tau}{d\lambda}\left(W_{nn}\mathcal{N}^2 + W_{n\bar{m}}\mathcal{N}\mathcal{M} + W_{\bar{m}\bar{m}}\mathcal{M}^2\right) \\ &= \sum_{k=-\infty}^{\infty}\sum_{n=-\infty}^{\infty} J_{\ell mkn}(\omega) e^{-i(k\Upsilon_\theta + n\Upsilon_r)\lambda}, \end{aligned} \tag{65}$$

where

$$J_{\ell mkn} = \int_0^{2\pi}\int_0^{2\pi} e^{i(k\phi_\theta + n\phi_r)} J_{\ell m\omega}(\phi_r, \phi_\theta) \frac{d\phi_\theta d\phi_r}{(2\pi)^2}, \tag{66}$$

with $\phi_r = \Upsilon_r\lambda$, $\phi_\theta = \Upsilon_\theta\lambda$ defined as the decoupled phases. Finally, we can rewrite the integral, with $\gamma = (-\infty, \infty)$, as

$$\begin{aligned} I &= \int_{-\infty}^{\infty} e^{i(\omega\Gamma - m\Upsilon_\varphi - k\Upsilon_\theta - n\Upsilon_r)\lambda} \sum_{k=-\infty}^{\infty}\sum_{n=-\infty}^{\infty} J_{\ell mkn}(\omega) d\lambda \\ &= \sum_{k=-\infty}^{\infty}\sum_{n=-\infty}^{\infty} 2\pi\delta(\omega\Gamma - m\Upsilon_\varphi - k\Upsilon_\theta - n\Upsilon_r) J_{\ell mkn}(\omega). \end{aligned} \tag{67}$$

Then, we insert it into Eq. (28) and Eq. (29) and obtain the gravitational waveform at infinity as

$$\begin{aligned} h &= h_+ - ih_\times \\ &= \frac{8}{r}\sum_{\ell m}\int_{-\infty}^{\infty} \frac{I}{2i\omega B^{\text{inc}}_{\text{SN}}} {}_{-2}S^{a\omega}_{\ell m}(\theta) e^{-i\omega(t-r_*) + im\varphi} d\omega \\ &= \sum_{\ell mnk} h_{\ell mnk}, \end{aligned} \tag{68}$$

where

$$\omega_{mnk} = m\frac{\Upsilon_\varphi}{\Gamma} + n\frac{\Upsilon_r}{\Gamma} + k\frac{\Upsilon_\theta}{\Gamma} \tag{69}$$

and

$$h_{\ell mnk} = -\frac{2\mu}{r}\frac{Z^\infty_{\ell mnk}}{\omega^2_{mnk}} {}_{-2}S^{a\omega_{mnk}}_{\ell m}(\theta) e^{-i\omega_{mnk}(t-r_*) + im\varphi}, \tag{70}$$

where

$$Z^\infty_{\ell mnk} = -\frac{4i\pi\omega_{mnk}}{B^{\text{inc}}_{\text{SN}}\Gamma} J_{\ell mnk}. \tag{71}$$

The averaged energy flux, angular momentum flux, and Carter constant flux at infinity are given by

$$\left\langle \dot{\mathcal{E}} \right\rangle^\infty = \sum_{\ell mnk} \frac{\left|Z^\infty_{\ell mnk}\right|^2}{4\pi\omega^2_{mnk}}, \tag{72a}$$

$$\left\langle \dot{\mathcal{L}}_z \right\rangle^\infty = \sum_{\ell mnk} \frac{m\left|Z^\infty_{\ell mnk}\right|^2}{4\pi\omega^3_{mnk}}, \tag{72b}$$

$$\left\langle \dot{\mathcal{Q}} \right\rangle^\infty = \sum_{\ell mnk} \frac{(\mathcal{L}_{mnk} + k\Upsilon_\theta)\left|Z^\infty_{\ell mnk}\right|^2}{2\pi\omega^3_{mnk}}, \tag{72c}$$

where

$$\mathcal{L}_{mnk} = m\langle\cot^2\theta\rangle\mathcal{L}_z - a^2\omega_{mnk}\langle\cos^2\theta\rangle\mathcal{E}, \tag{73a}$$

$$\langle\cot^2\theta\rangle = \frac{1}{\pi}\int_0^\pi \left[\cot\theta(\phi_\theta)\right]^2 d\phi_\theta, \tag{73b}$$

$$\langle\cos^2\theta\rangle = \frac{1}{\pi}\int_0^\pi \left[\cos\theta(\phi_\theta)\right]^2 d\phi_\theta. \tag{73c}$$

2. Unbound orbits

Unlike bound orbits, $\mathcal{W}(r \to \infty)$ and $\mathcal{W}'(r \to \infty)$ may not vanish for unbound orbits. An example of this would be the radial infall of a particle from infinity. In this case, the natural thing to do with our SN-IBP approach would be choosing $y_0 = y_1 = 0$ such that the boundary terms at infinity in Eq. (33) vanish, but one still needs to solve Eq. (20) to evaluate $\mathcal{W}(r = r_+)$ and $\mathcal{W}(r = r_+)$. While for the original formulation (without using IBP), we also need to solve for $\mathcal{W}(r)$ and integrate Eq. (26). Therefore, one needs to solve for $\mathcal{W}(r)$ either way, and our IBP approach does not have any advantage over the original formulation. A question naturally arises as to which method should be used for unbound orbits? We can answer this question by analyzing the convergence of the integrands in both formulations.

As an example, we derive how one calculates the waveform induced by a particle falling radially into a Kerr BH along its spin axis without using IBP in the original SN formulation. The 4-velocity is given by

$$u^t = \mathcal{E}\frac{r^2 + a^2}{\Delta}, \tag{74a}$$

$$u^r = -\frac{\sqrt{\mathcal{E}^2(r^2 + a^2)^2 - \Delta(r^2 + a^2\mathcal{E}^2)}}{r^2 + a^2}, \tag{74b}$$

$$u^\theta = u^\varphi = 0, \tag{74c}$$

where $\mathcal{E}$ is the orbital energy per mass. One instantly find that $\bar{\mathcal{M}} = 0$ from the definition in Eq. (37) and therefore only $\mathcal{W}_{nn}$ is nonvanishing.

Specifically, we see that when $\mathcal{E} = 1$, we have $u^r(r \to \infty) \sim \mathcal{O}(r^{-1/2})$ and therefore $\mathcal{W}(r \to \infty) \sim f_0 \sim \mathcal{O}(1/r^{1/2})$. When $\mathcal{E} > 1$, we have $u^r(r \to \infty) \sim \mathcal{O}(1)$ as $r \to \infty$ and therefore $\mathcal{W}(r \to \infty) \sim f_0 \sim \mathcal{O}(1)$.[5] By setting $y_0 = y_1 = 0$, we have $Y(r \to \infty) \sim \mathcal{O}(1/r)$. From the definition in Eq. (30) and Eq. (20), we already know that $Y''(r \to \infty) \sim \mathcal{O}(1/r^3)$, $\mathcal{W}''(r \to \infty) \sim \mathcal{O}(r^{1/2})$ for $\mathcal{E} = 1$, and $\mathcal{W}''(r \to \infty) \sim \mathcal{O}(1)$ for $\mathcal{E} > 1$. As a result, we obtain the convergence of the integrands in the SN-IBP and the original SN method, respectively, as

$$\begin{aligned} \text{SN-IBP:} \quad Y(r)\mathcal{W}''(r) &\sim \begin{cases} \mathcal{O}(1/r^{1/2}), & \mathcal{E} = 1 \\ \mathcal{O}(1/r), & \mathcal{E} > 1 \end{cases}, \\ \text{original SN:} \quad Y''(r)\mathcal{W}(r) &\sim \begin{cases} \mathcal{O}(1/r^{7/2}), & \mathcal{E} = 1 \\ \mathcal{O}(1/r^3), & \mathcal{E} > 1 \end{cases}. \end{aligned} \tag{75}$$

From Eq. (75), we conclude that the integrand of the non-IBP method converge way faster than that of the IBP method. So still suggest using the non-IBP method for unbound orbits. We will show the convergence speed clearly in Sec. III B.

[5] For $\mathcal{E} < 1$, the particle cannot escape to infinity, which reduces to the bound case.

For an unbound orbit, there is no discrete frequency spectrum as in the case for a bound orbit. The frequency domain waveform $\tilde{h}(\omega)$ and the now-continuous energy spectrum $d\mathcal{E}/d\omega$, in the case of radial infall, can be expressed as

$$\tilde{h}_\ell(\omega) = -\frac{2\mu}{r}\frac{Z^\infty_{\ell 0\omega}}{\omega^2}{}_{-2}S^{a\omega}_{\ell 0}(\theta) = \frac{8\mu}{r}\frac{X^\infty_{\ell 0\omega}}{c_0}{}_{-2}S^{a\omega}_{\ell 0}(\theta), \tag{76a}$$

$$\begin{aligned} \left(\frac{d\mathcal{E}}{d\omega}\right)^\infty_\ell &= \frac{\mu^2}{2\omega^2}\left(\left|Z^\infty_{\ell 0\omega}\right|^2 + \left|Z^\infty_{\ell 0-\omega}\right|^2\right) \\ &= 8\omega^2\mu^2\left(\left|\frac{X^\infty_{\ell 0\omega}}{c_0}\right|^2 + \left|\frac{X^\infty_{\ell 0-\omega}}{c_0}\right|^2\right). \end{aligned} \tag{76b}$$

The corresponding time-domain waveform is given by

$$h_+ - ih_\times = \sum_\ell \int_{-\infty}^{\infty} \tilde{h}_\ell(\omega)e^{-i\omega u}d\omega, \tag{77}$$

where $u = t - r_*$ is the retarded time.

III. RESULTS

In this section, we present some example waveforms and energy flux calculations for both bound and unbound orbits. Specifically, for bound orbits, we use the SN-IBP approach introduced in this paper to compute the EMRI waveform snapshot (à la Ref. [20]) for a generic timelike geodesic. For unbound orbits, we consider particles falling radially from infinity along the spin axis and covering two cases — the rest limit ($\mathcal{E} = 1$) and the ultra-relativistic limit ($\mathcal{E} \to \infty$).

A. Generic bound stable orbits

Numerous studies have already calculated the gravitational radiation from particles on bound Kerr geodesic orbits using the Teukolsky formalism, including eccentric-equatorial orbits [27], inclined-spherical orbits [28], and generic orbits [20]. Prior to this work, there were also calculations using the SN formalism on circular-equatorial orbits [29], eccentric-equatorial orbits [30], and inclined-spherical orbits [25]. No calculation for generic orbits has been done with the SN formalism. Here, we present our results and compare them with the literature and codes using the Teukolsky formalism, namely the `BHPToolkit` [31] and `pybhpt` [32, 33].

Here, we show the results of Eq. (70)-(72a). We set $a = 0.9M$, $p = 6.0M$, $e = 0.7$, $x = \cos\pi/4$ as our fiducial parameters for a generic geodesic orbit.[6] For higher values of n and k, Eq. (66) becomes a highly oscillatory double integral, which is hard to integrate numerically. To

[6] The trajectory is also visualized in Fig. 10 in Appendix E.

achieve a better precision and speed, we employ Levin's method, which converts a quadrature problem into an ODE problem. The algorithm is introduced in Appendix F.

To verify our codes, we calculate the energy flux using the SN-IBP method in this work (implemented in `GeneralizedSasakiNakamura.jl`[7]) and `pybhpt` for the $\ell = m = 2$ and $\ell = m = 4$ modes with $k = 0$ and $n = 0$ to $n = 70$ in Fig. 2. In addition, we tabulate the total

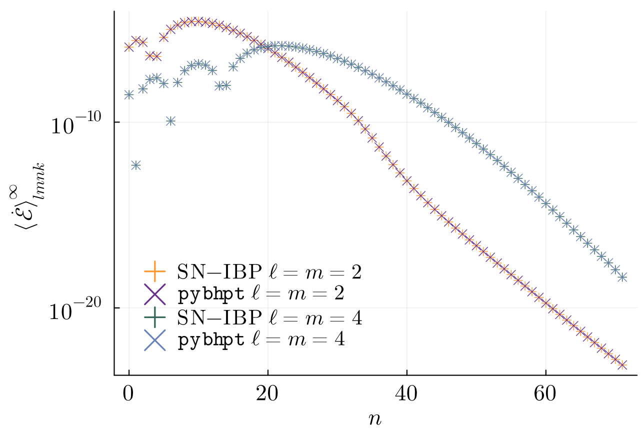

FIG. 2. The energy flux at infinity for $a = 0.9M$, $p = 6.0M$, $e = 0.7$, $x = \cos\pi/4$. The mode indexes are $\ell = m = 2$ and $\ell = m = 4$ with polar index $k = 0$ and radial index $n = 0$ to $n = 70$. The two approaches agree very well.

energy flux for each ℓ mode from the two codes, which is defined as

$$\left\langle \dot{\mathcal{E}} \right\rangle^{\infty}_{\ell} = \sum_{mnk} \left\langle \dot{\mathcal{E}} \right\rangle^{\infty}_{\ell mnk} . \tag{78}$$

The truncation rules[8] for the summation in Eq. (78) are specified as follows:

1. For each ℓ mode, we manually set the truncation limits as $n^{\ell}_{\max} = 40 + 10\ell$ and $k^{\ell}_{\max} = 8 + 2\ell$.
2. For fixed ℓ, m, and $n = 0$, if three consecutive values of $\langle\dot{\mathcal{E}}\rangle^{\infty}_{\ell mnk}$ are smaller than $10^{-6} \times \langle\dot{\mathcal{E}}\rangle^{\infty}_{\ell}$ (i.e., the current value of the summation of that ℓ mode), then we truncate the k summation.
3. For fixed ℓ, m, and k, if three consecutive values of $\langle\dot{\mathcal{E}}\rangle^{\infty}_{\ell mnk}$ are smaller than current $10^{-6} \times \langle\dot{\mathcal{E}}\rangle^{\infty}_{\ell}$ (i.e., current value of the summation of this ℓ mode), then we truncate the n summation.

Following these rules, we calculate the energy fluxes for the $\ell = 2$, 3, 4, 5, and 6 modes. These values are tabulated Tab. I, together with the total number of modes summed in those calculations.[9] The two sets of numbers agree to the tenth digit, and disagreement only appears after the eleventh digit (indicated by the brackets in Tab. I). Moreover, in Fig. 3, we show the waveform snapshot with the fiducial parameters, using the amplitude data from Tab. I. In total, 5869 modes were used om the generation of the waveform.

TABLE I. The energy fluxes of different ℓ modes for $a = 0.9M$, $p = 6.0M$, $e = 0.7$, $x = \cos\pi/4$. The last column is the total number of modes in the summation.

$\langle\dot{\mathcal{E}}\rangle^{\infty}_{\ell}$	SN-IBP	`pybhpt`	modes
$\ell = 2$	0.0006264593(7943)	0.0006264593(5842)	859
$\ell = 3$	0.0001785517(1276)	0.0001785517(2034)	1052
$\ell = 4$	0.0000631841(4574)	0.0000631841(7247)	1236
$\ell = 5$	0.0000244116(3861)	0.0000244116(6410)	1323
$\ell = 6$	0.0000096610(2419)	0.0000096610(4076)	1399

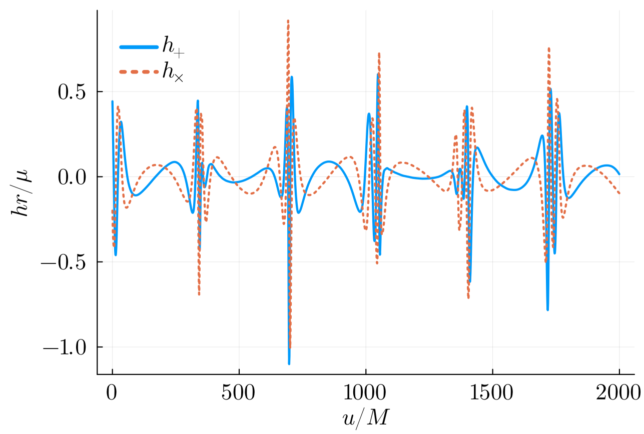

FIG. 3. The GW waveform snapshot for $a = 0.9M$, $p = 6.0M$, $e = 0.7$, $x = \cos\pi/4$ viewing at $\theta = \pi/2$ and $\varphi = 0$.

B. Radial infalls

As discussed in Sec. II C 2, there are two cases—$\mathcal{E} = 1$ where the particle has no initial velocity at infinity (also referred to as the rest limit) and $\mathcal{E} > 1$. In addition, $\mathcal{E} \gg 1$ or the ultra-relativistic limit corresponds to a particle moving nearly at the speed of light and hitting a Kerr BH along its spin axis.

The asymptotic behaviour of u^r at infinity differs in these two cases, leading to distinct asymptotic behaviours of $f_{0,1,2}$ in Eq. (47a). This further results in differences in the asymptotic behaviour of $\mathcal{W}(r)$ and the integrand within the Green's function integral involved

[7] https://github.com/ricokaloklo/GeneralizedSasakiNakamura.jl from v0.7.0 onwards.

[8] Note that we do not claim this set of truncation rules to be optimal.

[9] Note that in these calculations, both code use the same truncation strategy presented above.

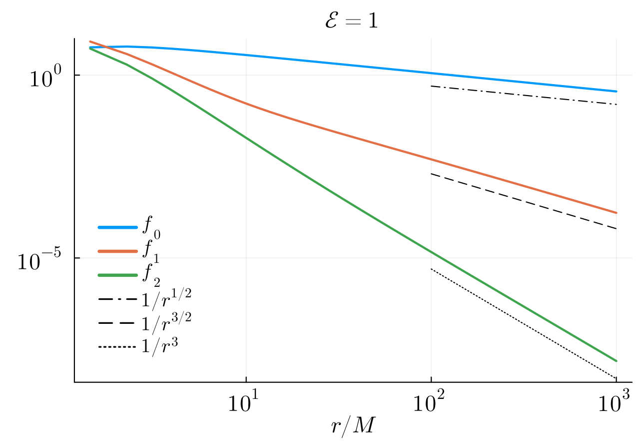

(a)

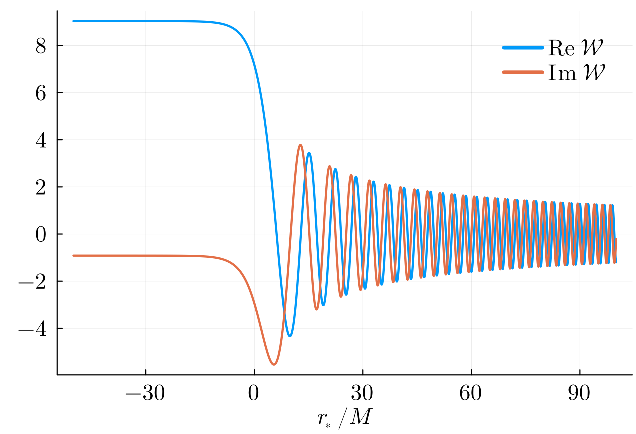

(b)

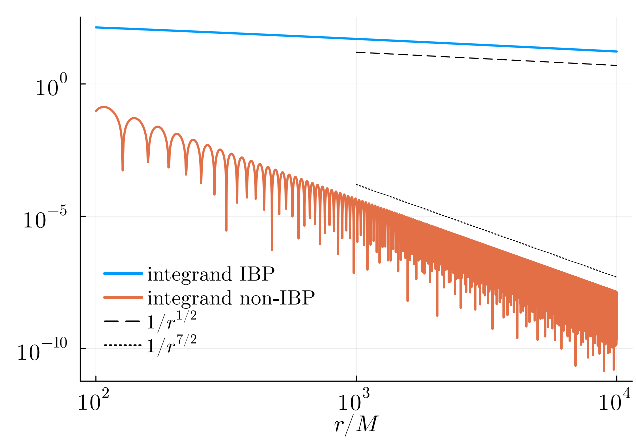

(c)

FIG. 4. The $\mathcal{E} = 1$ case. Panel (a) illustrates the variation of f_0, f_1, and f_2 with r. As $r \to \infty$, f_0 converges at a rate of $1/r^{1/2}$, f_1 converges at a rate of $1/r^{3/2}$, and f_2 converges at a rate of $1/r^3$. Panel (b) shows the variation of the $\mathcal{W}(r_*)$ function. It converges at the same rate as f_0, i.e. $1/r^{1/2}$, and its oscillation frequency increases with increasing r_*. Panel (c) presents the magnitudes of the integrands in the Green's function integrals for the IBP and non-IBP methods. The IBP method defined in Eq. (36) exhibits a convergence rate of $1/r^{1/2}$, while the non-IBP (i.e., the original SN) method defined in Eq. (26) converges faster as $1/r^{7/2}$. Other parameters are $\ell = 2$, $m = 0$, $a/M = 0.9$, and $M\omega = 0.5$.

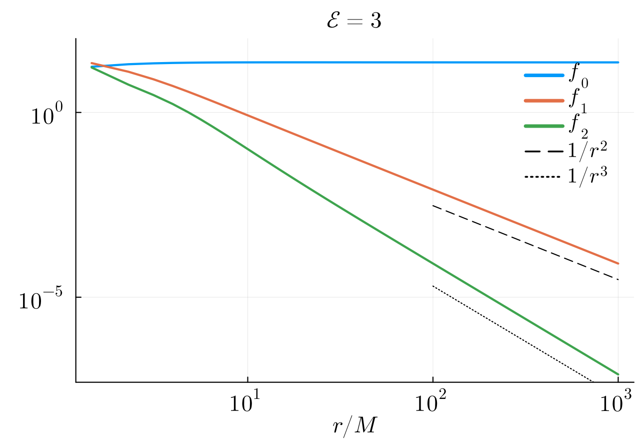

(a)

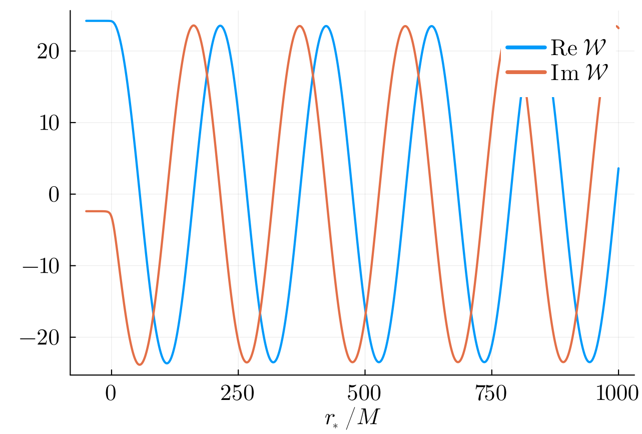

(b)

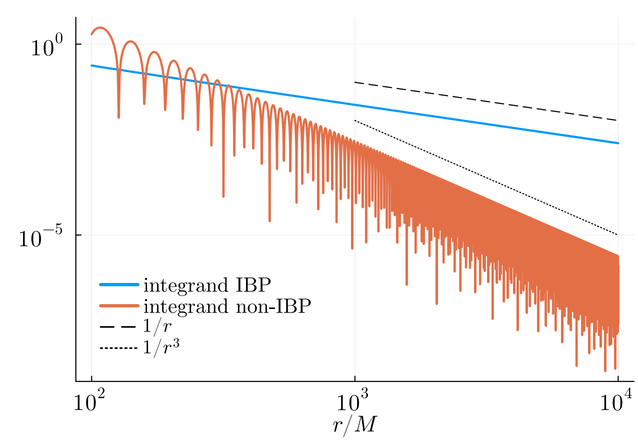

(c)

FIG. 5. The same as Fig. 4, but with $\mathcal{E} = 3$.

in the calculations. Consequently, the results obtained for these two cases are also significantly different. The behaviours of $f_{0,1,2}$, $\mathcal{W}$ and the Green's function integrand are shown in Fig. 4 for $\mathcal{E} = 1$ and Fig. 5 for $\mathcal{E} = 3$. One can see that $f_0 \sim \mathcal{O}(1/r^{1/2})$, $f_1 \sim \mathcal{O}(1/r^{3/2})$, $f_2 \sim \mathcal{O}(1/r^3)$ for $\mathcal{E} = 1$ and $f_0 \sim \mathcal{O}(1)$, $f_1 \sim \mathcal{O}(1/r^2)$,

$f_2 \sim \mathcal{O}(1/r^3)$ for $\mathcal{E} > 1$.

Since the convergence of $\mathcal{W}$ is controlled by f_0 following Eq. (47a), therefore the overall convergence of the integrand for the original SN formulation [cf Eq. (26)] is $\sim \mathcal{O}(1/r^{7/2})$ for $\mathcal{E} = 1$ and $\sim \mathcal{O}(1/r^3)$ for $\mathcal{E} > 1$. However, the integrand in the SN-IBP approach in Eq. (36) behaves as $\sim \mathcal{O}(1/r^{1/2})$ for $\mathcal{E} = 1$ and $\sim \mathcal{O}(1/r)$ for $\mathcal{E} > 1$. All of the asymptotic behaviours above agree with our theoretical analyses in Sec. II C 2.

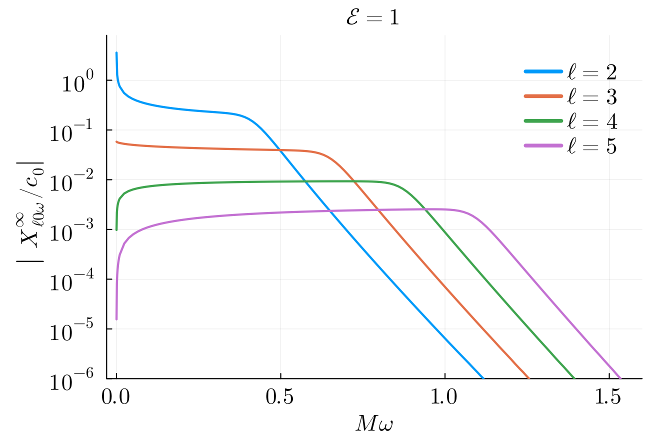

(a)

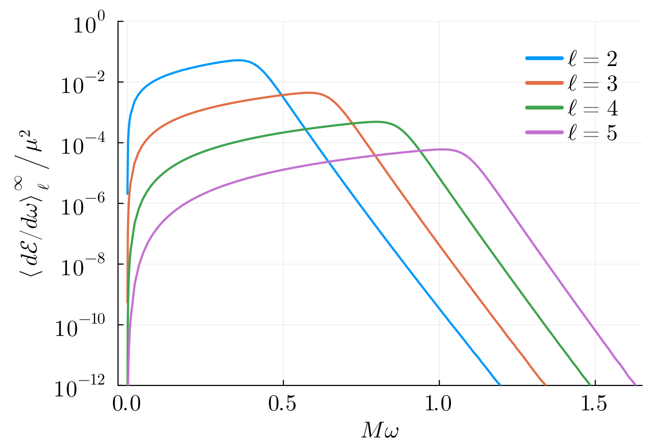

(b)

FIG. 6. The amplitude and energy spectrum of GW induced by a particle falling radially into a Kerr BH along its spin axis with zero initial velocity ($\mathcal{E} = 1$) at infinity. The amplitude is normalized by μ and the energy spectrum is normalized by μ^2. Other parameters are $a = 0.9M$ and $m = 0$.

Figures 6 and 7 show the amplitude $|X^\infty_{\ell 0\omega}/c_0|$ and energy spectrum $(d\mathcal{E}/d\omega)^\infty_\ell$ in rest limit and the ultra-relativistic limit (using $\mathcal{E} = 100$ as an approximation), respectively. We can see that Fig. 6 agrees well with Fig. 1 in Ref. [34], which shows the amplitude and the energy spectrum for a radial infall into a Schwarzchild BH in the rest limit. We also find the same power-law behaviour of the amplitudes as

$$\left|\frac{X^\infty_{\ell 0\omega}}{c_0}\right| \sim \omega^{(\ell-3)/3} \tag{79}$$

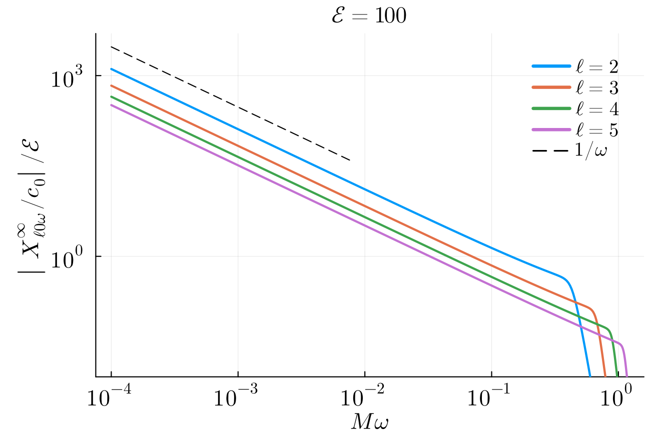

(a)

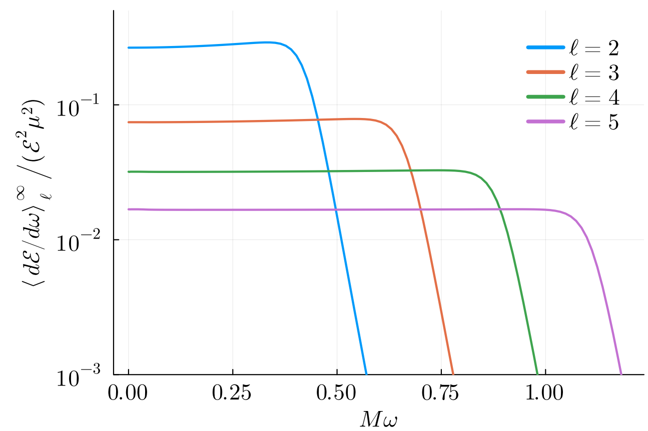

(b)

FIG. 7. The amplitude and energy spectrum of GW induced by a particle falling radially into a Kerr BH along its spin axis in the ultra-relativistic limit (we set $\mathcal{E} = 100$). The amplitude is normalized by $\mu\mathcal{E}$ and the energy spectrum is normalized by $\mu^2\mathcal{E}^2$. Other parameters are $a = 0.999M$ and $m = 0$.

at the zero frequency limit (ZFL), i.e. $\omega \to 0$, consistent with the result reported in Ref. [34]. In the ultra-relativistic limit, one can see from Fig. 7 that the power-law behaviour of all the ℓ modes are

$$\left|\frac{X^\infty_{\ell 0\omega}}{c_0}\right| \sim 1/\omega \tag{80}$$

at the ZFL. This makes the energy spectra nonvanishing at the ZFL by definition in Eq. (76).

Therefore, we can extract the value for the energy spectrum values in the ZFL per ℓ mode numerically from our calculations. Theoretically, the total energy spectrum (summed over all ℓ modes) in the ZFL was derived in Ref. [35], which is given by

$$\left(\frac{d\mathcal{E}}{d\omega}\right)^{\mathrm{ZFL}} = \sum_{\ell=2}^{\infty}\left(\frac{d\mathcal{E}}{d\omega}\right)^{\mathrm{ZFL}}_\ell = \frac{4}{3\pi}\mathcal{E}^2\mu^2, \tag{81}$$

while the per-ℓ mode value was also given in Ref. [36] as

$$\left(\frac{d\mathcal{E}}{d\omega}\right)^{\rm ZFL}_{\ell} = \frac{4\mathcal{E}^2\mu^2}{\pi}\frac{(2\ell+1)(\ell-2)!}{(\ell+2)!}. \qquad (82)$$

Here we show the numerical values extracted from Fig. 7(b) and the theoretical predictions using Eq. (82). The results are tabulated in Tab. II. Our numerical results match the theoretical results within an error of 0.1% and are consistent with those shown in Ref. [37].

TABLE II. The numerical and theoretical ZFL values of the energy spectrum in the ultra-relativistic limit, normalized by $\mathcal{E}^2\mu^2$.

$\langle d\mathcal{E}/d\omega\rangle^{\rm ZFL}_{\ell}$	numerical result	theoretical prediction
$\ell=2$	0.26524876	0.26525824
$\ell=3$	0.07422927	0.07427231
$\ell=4$	0.03180048	0.03183099
$\ell=5$	0.01668822	0.01667338

Finally, we show in Fig. 8 the time-domain waveform in the rest limit by performing an inverse FT in Eq. (77).

IV. DISCUSSIONS

A. Waveform modeling for extreme mass ratio inspirals

One obvious application of our SN-IBP approach would be computing EMRI waveforms, which we have already demonstrated in Sec. III A (and Fig. 3). However, such waveform generation requires many—around thousands of—modes to be calculated and summed up, which can take upwards of seconds per waveform and thus too slow for the purpose of LISA data analysis.

Fortunately, the FastEMRIWaveforms framework [38–41] solves this problem by generating EMRI waveforms using precomputed waveform amplitude and flux data and thus decouples the waveform generation for data analysis from the relatively expensive waveform calculation. As mentioned in Ref. [41], the framework can be easily extended handle eccentric and inclined orbits around a Kerr BH once the corresponding amplitude and flux data are available, which we can easily generate with the SN-IBP approach.

Since our formalism and code implementation are independent from the Teukolsky formalism, one can also use our code to cross-validate the adiabatic—or 0PA—amplitude and flux data in the literature. In terms of performance, our implementation is comparable with the state-of-the-art `pybhpt`. We benchmark the performance of three different codes on calculating the waveform amplitude at infinity using the same set of fiducial parameters, i.e., $a=0.9M$, $p=6.0M$, $e=0.7$, $x=\cos\pi/4$, that are used throughout the paper, namely ours, `BHPToolkit`, and `pybhpt`. The single-core CPU times are tabulated in Tab. III.[10] Note that no attempt was made to optimize our current implementation, and there is still room for improvement. For example, the current bottleneck of the calculation is actually in solving the homogeneous solutions $X^{\rm in,up}$. Optimization of our implementation is planned but it is outside the scope of this paper.

TABLE III. Runtime comparison using three different codes calculating the waveform amplitude at infinity with the same set of fiducial parameters $a=0.9M$, $p=6.0M$, $e=0.7$, $x=\cos\pi/4$ that are used throughout the paper. Some of the computations using the `Mathematica` package from `BHPToolkit` were aborted after running for half an hour.

(ℓ,m,n,k)	this work [ms]	`BHPToolkit` [ms]	`pybhpt` [ms]
$(2,2,0,0)$	54	6.44×10^4	45
$(2,2,0,5)$	53	2.31×10^5	63
$(2,2,10,0)$	58	1.96×10^5	48
$(2,2,50,0)$	83	Aborted	389
$(4,4,0,0)$	68	4.93×10^4	53
$(4,4,0,5)$	73	1.79×10^5	47
$(4,4,10,0)$	70	2.94×10^5	54
$(4,4,50,0)$	205	Aborted	398

B. Current limitations and future extensions

While the IBP approach we presented here drastically simplifies the computation of the waveform amplitude and fluxes at infinity for bound orbits when using the SN formalism, there are still some limitations to our formulation. For instance, the IBP approach has no advantage in computing those quantities near the BH horizon over the original formulation. This is because, when near the horizon (or $r\to r_+$), the inverse transformation from the SN variable to the Teukolsky variable [cf Eq. (16)] is, in fact, dominated by the contribution coming from $\mathcal{S}$ when using the canonical solution $\mathcal{W}^{\rm canonical}$ (and by extension $\mathcal{S}^{\rm canonical}$). Therefore, we still need to compute $\mathcal{W}(r=r_+)$ when computing fluxes down the horizon.

Note that the SN formalism itself is perfectly valid in this case. In fact, one can choose $w_{0,1}$ [cf Eq. (53) in Sec. II B 3] such that it is the contribution coming from the Λ^{-1} operator acting on the inhomogeneous SN solution that dominates the transformation [26]. However, we have already imposed the boundary conditions that $w_{0,1}=0$ to make the boundary terms in Eq. (33) at infinity vanish. A workaround to this issue is to solve for the inhomogeneous solution with a spin weight of $s=+2$ instead, which allows us to still use the IBP approach to simplify calculations. We leave this for an upcoming publication.

[10] The benchmarking was done with an Apple M2 chip.

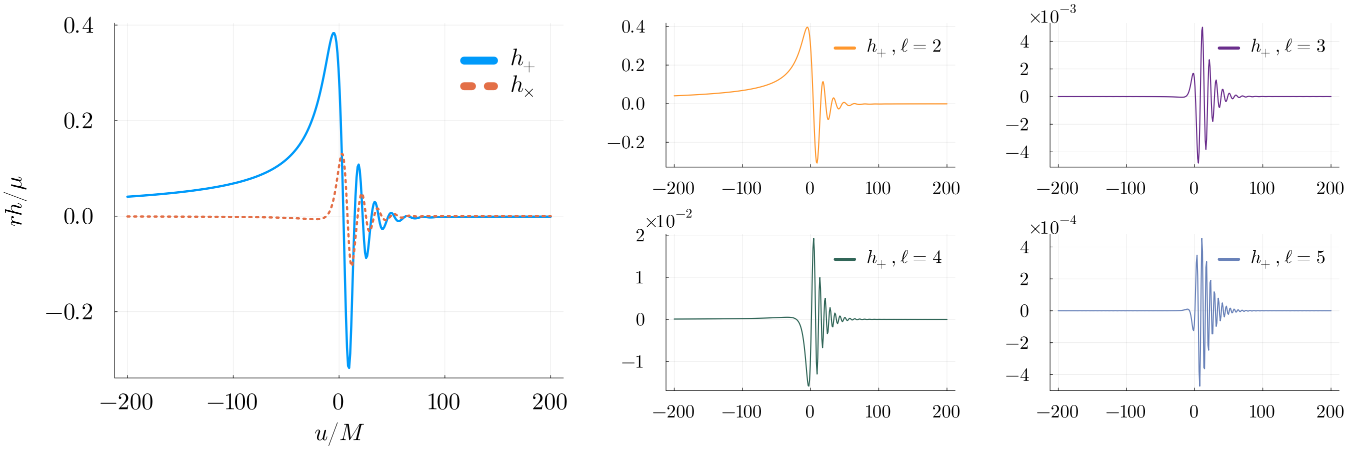

FIG. 8. The GW waveform of the radial infall for $\mathcal{E} = 1$ viewing at $\theta = \pi/2$ and $\varphi = 0$. The left panel shows the summation $h_+ - ih_\times = h_2 + h_3 + h_4 + h_5$. The right panel show the waveforms of the separate modes.

Another extension to our work here is to consider also generic plunge orbits into a Kerr BH. We believe that the IBP approach is still advantageous over the original SN formulation. These kind of problems also serve as an analytical model for studying and understanding more about the physics and mechanism of quasinormal mode excitation in binary black hole mergers using the SN formalism [23, 42, 43]. We again leave this for a future publication.

V. CONCLUSIONS

In this work, we introduce a new scheme for solving the inhomogeneous SN equation using integration by parts. When computing gravitational waveforms and fluxes at infinity coming from Kerr BHs perturbed by particles in bound orbits, this simple trick eliminates the need for performing yet another radial integration to obtain the source term that needs to be convolved with a Green's function as in the original SN formulation. Our approach enables the efficient computation of gravitational waveforms within the SN formalism now in *all* cases, from bound to unbound orbits, without having to transform between the Teukolsky and SN formalisms in intermediate steps.

Specifically, we define a new auxiliary variable Y in place of the SN variable X that we convolve with the source term $\mathcal{T}$ that one would use in the Teukolsky formalism. This new variable Y is independent of the source term and therefore only needs to be computed once per frequency. Furthermore, it is nonoscillatory and regular at the BH horizon and spatial infinity, thus allowing for easy numerical calculations. As a byproduct of this work, we also derive a source term for the SN formalism that is valid for arbitrary motion and not just for geodesic motions.

We demonstrate that our approach and code implementation yield waveform amplitude and flux data that are consistent with the literature, while already achieving comparable speed without any optimization attempt. Getting these amplitude and flux data accurately and efficiently is crucial as they enable the rapid generation of waveforms for future LISA data analysis, especially for EMRI waveforms with generic (eccentric and inclined) bound orbits.

ACKNOWLEDGMENTS

The Center of Gravity is a Center of Excellence funded by the Danish National Research Foundation under grant no. DNRF184. This work was supported by the research Grants No. VIL37766 and No. VIL53101 from Villum Fonden, and the DNRF Chair program Grant No. DNRF162 by the Danish National Research Foundation. This work has received funding from the European Union's Horizon 2020 research and innovation program under the Marie Sklodowska-Curie Grant Agreement No. 101131233. This work received no direct support from the National Natural Science Foundation of China. XC acknowledges support from the NSFC Grant No. 12473037. Additionally, RKLL would like to thank KIAA at Peking University for their hospitality during his visit and Norichika Sago for his help in the early stage of this work.

DATA AVAILABILITY

A Mathematica notebook deriving and storing expressions shown here is publicly available from the Zenodo repository [44].

Appendix A: Deriving the relation between the Teukolsky and Sasaki-Nakamura source terms

In this Appendix, we re-derive the relation between the Teukolsky source term $\mathcal{T}$ and the SN source term $\mathcal{S}$ following Refs. [17, 18].

We first consider the variable $\mathcal{X}$, which is related to the SN variable X by $X(r) = \sqrt{(r^2+a^2)/\Delta^2}\mathcal{X}$ (cf Ref. [13]). It satisfies a Regge-Wheeler-like equation given by

$$\Delta^2\left(\frac{1}{\Delta}\mathcal{X}'\right)' - \Delta F_1\mathcal{X}' - U_1\mathcal{X} = \mathscr{S}, \tag{A1}$$

where $\mathscr{S}$ is the source term for the $\mathcal{X}$ variable. Note that this equation reduces to the usual Regge-Wheeler equation when $a = 0$ since in this case $\eta(r) = c_0$ is just a constant. We use Eq. (A1) to write $\mathcal{X}''$ in terms of $\mathcal{X}$ and $\mathcal{X}'$, which is

$$\mathcal{X}'' = \frac{\mathscr{S}}{\Delta} + \frac{U_1}{\Delta}\mathcal{X} + \left[F_1 + \frac{\Delta'}{\Delta}\right]\mathcal{X}', \tag{A2}$$

where setting $\mathscr{S} = 0$ recovers the source-less case.

Following Refs. [17, 18], we *modify* the inverse transformation from SN variables X to Teukolsky variables R as

$$R = \frac{1}{\eta}\left[\left(\alpha + \frac{\beta'}{\Delta}\right)\mathcal{X} - \frac{\beta}{\Delta}\mathcal{X}'\right] + \frac{\mathscr{S}}{\eta}, \tag{A3}$$

and setting $\mathscr{S} = 0$ recovers the homogeneous case.

We then evaluate R' in terms of $\mathcal{X}$ and $\mathscr{S}$ (and their derivatives) and substitute them back to the inhomogeneous Teukolsky equation in Eq. (3). As a result, we obtain an ODE for $\mathscr{S}$, which is given by

$$\begin{aligned}&\Delta^2\left[\frac{1}{\Delta}\left(\frac{\mathscr{S}}{\eta}\right)'\right]' \\ &+ \Delta^2\left[-\frac{\beta}{\Delta^3}\left(\frac{\mathscr{S}}{\eta}\right)\right]' + (\alpha - V_{\mathrm{T}})\frac{\mathscr{S}}{\eta} = -\mathcal{T}.\end{aligned} \tag{A4}$$

Our goal is to solve for $\mathscr{S}$ in terms of $\mathcal{T}$. Note that we can rewrite Eq. (A4) into a much more compact form as

$$\mathscr{J}^{\dagger}\left[\mathscr{J}^{\dagger}\left(\frac{r^2}{\Delta}\frac{\mathscr{S}}{\eta}\right)\right] = -\frac{r^2}{\Delta^2}\mathcal{T}, \tag{A5}$$

where $\mathscr{J}^{\dagger} \equiv \partial_r + iK/\Delta$ is a differential operator.[11] If we introduce an auxiliary variable $\mathcal{W}$ such that

$$\mathcal{W}(r) = f(r)\exp\left(\int^r i\frac{K}{\Delta}d\tilde{r}\right), \tag{A6}$$

for any differentiable function $f(r)$, then $\mathcal{W}'$ can be written as

$$\mathcal{W}'(r) = \exp\left(\int^r i\frac{K}{\Delta}d\tilde{r}\right)\mathscr{J}^{\dagger}[f(r)]. \tag{A7}$$

If we define

$$\mathcal{W}(r) = \frac{r^2}{\Delta}\frac{\mathscr{S}}{\eta}\exp\left(\int^r i\frac{K}{\Delta}d\tilde{r}\right), \tag{A8}$$

then by using the identity in Eq. (A7) twice, we have

$$(\mathcal{W}')' = \exp\left(\int^r i\frac{K}{\Delta}d\tilde{r}\right)\mathscr{J}^{\dagger}\left[\mathscr{J}^{\dagger}\left(\frac{r^2}{\Delta}\frac{\mathcal{S}}{\eta}\right)\right]. \tag{A9}$$

Using Eq. (A5), we have

$$\mathcal{W}'' = -\frac{r^2}{\Delta^2}\mathcal{T}\exp\left(\int^r i\frac{K}{\Delta}d\tilde{r}\right), \tag{20}$$

which is the ODE that one needs to solve to obtain $\mathscr{S}$ from $\mathcal{T}$.

Given the source term $\mathscr{S}$ for the variable $\mathcal{X}$, we can convert that to the source term needed the SN equation $\mathcal{S}$ simply with

$$\mathcal{S} = \frac{1}{(r^2+a^2)^{3/2}}\mathscr{S}, \tag{A10}$$

as $\mathcal{X}$ solutions are related to the corresponding X solutions by $X = \sqrt{(r^2+a^2)/\Delta^2}\mathcal{X}$. Putting everything together and the subscript back, we have

$$\mathcal{S}_{\ell m\omega} = \frac{\eta\Delta\mathcal{W}}{(r^2+a^2)^{3/2}r^2}\exp\left(-i\int^r\frac{K}{\Delta}d\tilde{r}\right). \tag{19}$$

Appendix B: The A terms and W terms

The source term components A in the Teukolsky formalism are given by

$$A_{nn0} = \frac{\mathscr{A}}{2}\rho\bar{\rho}^2\mathcal{N}^2\mathscr{L}_1^{\dagger}\left[\rho^{-4}\mathscr{L}_2^{\dagger}\left(\rho^3 S\right)\right], \tag{B1a}$$

$$A_{n\bar{m}0} = \mathscr{A}\bar{\rho}^2\mathcal{N}\bar{\mathcal{M}}\left[\left(\mathscr{L}_2^{\dagger}S\right)\left(\frac{iK}{\Delta} - \rho - \bar{\rho}\right) - a\sin\theta S\frac{K}{\Delta}(\rho - \bar{\rho})\right], \tag{B1b}$$

$$A_{\bar{m}\bar{m}0} = \frac{\mathscr{A}}{2}\bar{\rho}^2\bar{\mathcal{M}}^2 S\left[-i\left(\frac{K}{\Delta}\right)_{,r} - \frac{K^2}{\Delta^2} - 2i\rho\frac{K}{\Delta}\right], \tag{B1c}$$

$$A_{n\bar{m}1} = \mathscr{A}\bar{\rho}^2\mathcal{N}\bar{\mathcal{M}}\left[\mathscr{L}_2^{\dagger}S + ia\sin\theta(\rho - \bar{\rho})S\right], \tag{B1d}$$

$$A_{\bar{m}\bar{m}1} = \mathscr{A}\bar{\rho}^2\bar{\mathcal{M}}^2 S\left(i\frac{K}{\Delta} - \rho\right), \tag{B1e}$$

$$A_{\bar{m}\bar{m}2} = \frac{\mathscr{A}}{2}\bar{\rho}^2\bar{\mathcal{M}}^2 S, \tag{B1f}$$

[11] The $\mathscr{J}^{\dagger}$ and $\mathscr{J}$ operators are identical to the J_+ and J_- defined in Ref. [13], respectively.

where S are the SWSH with all of its subscripts suppressed to avoid confusion.

The source term components in the SN formalism are given by

$$W_{nn} = \mathscr{A}\frac{\rho\bar{\rho}^2}{2}\mathscr{L}_1^{\dagger}\left[\rho^{-4}\mathscr{L}_2^{\dagger}\left(\rho^3 S\right)\right] r^2 Y \,\text{phase}, \tag{B2a}$$

$$\begin{aligned} W_{n\bar{m}} = & -\mathscr{A} r\bar{\rho}^2 \left\{\left(\mathscr{L}_2^{\dagger} S\right)(\rho+\bar{\rho}) rY \right. \\ & \left. + \left[\mathscr{L}_2^{\dagger} S + ia\sin\theta\,(\rho-\bar{\rho})\,S\right](2Y + rY')\right\}\text{phase}, \end{aligned} \tag{B2b}$$

$$\begin{aligned} W_{\bar{m}\bar{m}} = & \mathscr{A} S\bar{\rho}^2 \left[\frac{X}{2\sqrt{r^2+a^2}} + (Y + 2rY')\,\text{phase} \right. \\ & \left. + \rho r\,(2Y + rY')\,\text{phase}\right], \end{aligned} \tag{B2c}$$

$$\begin{aligned} \text{phase} &= \exp\left(i\int^r \frac{K}{\Delta} d\tilde{r}\right) \\ &= \exp\left(i\omega r_* - \frac{iam}{2\sqrt{1-a^2}}\ln\frac{r-r_+}{r-r_-}\right). \end{aligned} \tag{B2d}$$

1. Normalization conventions

The value of the constant $\mathscr{A}$ above depends on the normalization conventions on the FT and SWSHs adopted. Specifically for the FT, there are canonically two conventions for the normalization, namely the unitary FT convention where

$$\begin{aligned} F(\omega) &= \frac{1}{\sqrt{2\pi}}\int_{-\infty}^{\infty} f(t)e^{i\omega t}dt, \\ f(t) &= \frac{1}{\sqrt{2\pi}}\int_{-\infty}^{\infty} F(\omega)e^{-i\omega t}d\omega, \end{aligned} \tag{B3}$$

and the non-unitary FT convention where

$$\begin{aligned} F(\omega) &= \frac{1}{2\pi}\int_{-\infty}^{\infty} f(t)e^{i\omega t}dt, \\ f(t) &= \int_{-\infty}^{\infty} F(\omega)e^{-i\omega t}d\omega. \end{aligned} \tag{B4}$$

As for SWSHs, there are also two normalization conventions where either

$$\int_0^{\pi} \left|{}_sS_{\ell m}^{a\omega}(\theta)\right|^2 \sin\theta d\theta = 1, \tag{B5}$$

which we will refer to as the SWSH normalization scheme 1, and

$$\int_0^{\pi} \left|{}_sS_{\ell m}^{a\omega}(\theta)\right|^2 \sin\theta d\theta = \frac{1}{2\pi}, \tag{B6}$$

which we will refer to as the SWSH normalization scheme 2, respectively.

Table IV shows the value of $\mathscr{A}$ with different choices of normalization conventions. Although the exact choice does not have any impact on physics, care should be taken when comparing results from different papers since the value of $\mathscr{A}$ may vary literature to literature. In this work, we use the non-unitary FT convention and the SWSH normalization scheme 2, and therefore $\mathscr{A} = -1$.

TABLE IV. The value of the constant $\mathscr{A}$ for different choices of FT and SWSH conventions. In this work, we have $\mathscr{A} = -1$.

$\mathscr{A}$	SWSH scheme 1	SWSH scheme 2
Unitary FT	$-1/\sqrt{2\pi}$	$-\sqrt{2\pi}$
Non-unitary FT	$-1/2\pi$	-1

Appendix C: Asymptotic expansions for $Y^{\text{in,up}}$

In this Appendix, we derive the asymptotic expansions for $Y^{\text{in,up}}$, respectively, for speeding up the numerical integration of Eq. (30), which is repeated here for reference as

$$Y_{\ell m\omega}^{\text{in/up}}{}''(r) \equiv \frac{X_{\ell m\omega}^{\text{in/up}}(r)}{r^2\sqrt{r^2+a^2}}\exp\left(-i\int^r \frac{K}{\Delta}dr\right). \tag{30}$$

1. The Y^{in} solution

Recall that in Ref. [13], we have shown that asymptotically as $r \to \infty$,

$$X^{\text{in}}(r\to\infty) = B_{\text{SN}}^{\text{ref}} e^{i\omega r_*}\sum_{w=0}^{\infty}\frac{\mathcal{C}_{+,w}^{\infty}}{r^w} + B_{\text{SN}}^{\text{inc}} e^{-i\omega r_*}\sum_{w=0}^{\infty}\frac{\mathcal{C}_{-,w}^{\infty}}{r^w}. \tag{C1}$$

The expressions of $\mathcal{C}_{\pm,1,2,3}^{\infty}$ can be found in the Appendix G of Ref. [13] (note that $\mathcal{C}_{\pm,0}^{\infty} = 1$). To write down an asymptotic expansion of $Y^{\text{in}}(r\to\infty)$, we also need the series expansions of the two other terms, which are given by

$$\exp\left(-i\int^r\frac{K}{\Delta}d\tilde{r}\right) = e^{-i\omega r_*}\sum_{j=0}^{\infty}\frac{a_j}{r^j}, \tag{C2a}$$

$$\frac{1}{r^2\sqrt{r^2+a^2}} = \frac{1}{r^3}\sum_{j=0}^{\infty}\frac{b_j}{r^j}, \tag{C2b}$$

where

$$a_j = \frac{1}{j!}B_j(P_1,\ldots,P_j), \tag{C3a}$$

$$P_j = \frac{iam\left(r_+^j - r_-^j\right)\Gamma(j)}{r_- - r_+}, \tag{C3b}$$

$$b_j = \frac{1+(-1)^j}{2}a^j\binom{-1/2}{j/2}, \tag{C3c}$$

and B_j denotes the j-th complete exponential Bell polynomial. Therefore, the piece that is proportional to $B_{\text{SN}}^{\text{ref}}$, which we denote as $Y_+^{\mathrm{in}\prime\prime}(r \to \infty)$, can be expressed as

$$\begin{aligned}
&Y_+^{\mathrm{in}\prime\prime}(r \to \infty) \\
=&\frac{X_+^{\infty}(r)}{r^2\sqrt{r^2+a^2}} \exp\left(-i\int^r \frac{K}{\Delta} d\tilde{r}\right) \\
=&\frac{B_{\mathrm{SN}}^{\mathrm{ref}}}{r^3}\left(\sum_{j=0}^{\infty}\frac{a_j}{r^i}\right)\left(\sum_{v=0}^{\infty}\frac{b_v}{r^j}\right)\left(\sum_{w=0}^{\infty}\frac{\mathcal{C}_{+,w}^{\infty}}{r^k}\right) \\
=&B_{\mathrm{SN}}^{\mathrm{ref}}\sum_{j=0}^{\infty}\frac{Y_j^{\infty,+}}{r^{j+3}},
\end{aligned} \tag{C4}$$

where

$$Y_{+,j}^{\infty} = \sum_{v=0}^{j}\sum_{w=0}^{j-v} a_v b_w \mathcal{C}_{+,j-v-w}^{\infty}. \tag{C5}$$

Notice that it is not oscillatory because $e^{-i\int^r \frac{K}{\Delta}d\tilde{r}} \sim e^{-i\omega r_*}$ [cf Eq. (B2d)] cancels out the phase term $e^{i\omega r_*}$ coming from X^{in}.

The other piece that is proportional to $B_{\mathrm{SN}}^{\mathrm{inc}}$, which we denote as $Y_-^{\mathrm{in}\prime\prime}(r \to \infty)$, is more complicated because the phase terms do not cancel out each other. Here, we need to expand also $r_*(r \to \infty)$, which is given by

$$r_* = r + 2\ln\frac{r}{2} - \sum_{v=1}^{\infty}\frac{2}{vr^v}\left(\sum_{j=0}^{v} r_+^j r_-^{v-j}\right). \tag{C6}$$

Therefore, we have

$$e^{-2i\omega r_*} = e^{4i\omega\ln 2}\frac{e^{-2i\omega r}}{r^{4i\omega}}\sum_{j=0}^{\infty}\frac{d_j}{r^j}, \tag{C7}$$

where

$$d_j = \frac{1}{j!}B_j(Q_1,\ldots,Q_j), \tag{C8a}$$

$$Q_j = 4i\omega\Gamma(j)\left(\sum_{v=0}^{j} r_+^v r_-^{j-v}\right). \tag{C8b}$$

Finally, we have

$$\begin{aligned}
&Y_-^{\mathrm{in}\prime\prime}(r \to \infty) \\
=&B_{\mathrm{SN}}^{\mathrm{inc}}\frac{e^{4i\omega\ln 2-2i\omega r}}{r^{3+4i\omega}}\left(\sum_{j=0}^{\infty}\frac{a_j}{r^j}\right)\left(\sum_{w=0}^{\infty}\frac{b_w}{r^w}\right) \\
&\left(\sum_{v=0}^{\infty}\frac{\mathcal{C}_{-,v}^{\infty}}{r^v}\right)\left(\sum_{u=0}^{\infty}\frac{d_u}{r^u}\right) \\
=&B_{\mathrm{SN}}^{\mathrm{inc}}\frac{e^{4i\omega\ln 2-2i\omega r}}{r^{4i\omega}}\sum_{j=0}^{\infty}\frac{Y_{-,j}^{\infty}}{r^{j+3}},
\end{aligned} \tag{C9}$$

where

$$Y_{-,j}^{\infty} = \sum_{v=0}^{j}\sum_{w=0}^{j-v}\sum_{u=0}^{j-v-w} a_v b_w \mathcal{C}_{-,u}^{\infty} d_{j-v-w-u}. \tag{C10}$$

Combining Eq. (C4) and Eq. (C9), we obtain Eq. (38).

It is not difficult to show that $Y_{+,0}^{\infty} = Y_{-,0}^{\infty} = 1$. Here, we also give the explicit expressions of the next three coefficients, which are given by

$$Y_{+,1}^{\infty} = \mathcal{C}_{+,1}^{\infty} - iam, \tag{C11a}$$

$$Y_{+,2}^{\infty} = \mathcal{C}_{+,2}^{\infty} - iam\mathcal{C}_{+,1}^{\infty} - \frac{a}{2}\left(a + am^2 + 2im\right), \tag{C11b}$$

$$Y_{+,3}^{\infty} = \mathcal{C}_{+,3}^{\infty} - iam\mathcal{C}_{+,2}^{\infty} - \frac{a}{2}\left(a + am^2 + 2im\right)\mathcal{C}_{+,1}^{\infty} + \frac{iam}{6}\left[a^2\left(m^2+5\right) + 6iam - 8\right], \tag{C11c}$$

$$Y_{-,1}^{\infty} = \mathcal{C}_{-,1}^{\infty} - iam + 8i\omega, \tag{C11d}$$

$$Y_{-,2}^{\infty} = \mathcal{C}_{-,2}^{\infty} - i\left(am - 8\omega\right)\mathcal{C}_{-,1}^{\infty} - \frac{1}{2}a^2\left(m^2 + 4i\omega + 1\right) + am(8\omega - i) + 8\omega(-4\omega + i), \tag{C11e}$$

$$\begin{aligned}
Y_{-,3}^{\infty} = &\mathcal{C}_{-,3}^{\infty} - i\left(am - 8\omega\right)\mathcal{C}_{-,2}^{\infty} + \frac{1}{2}\left[2am(8\omega - i) + 16\omega(i - 4\omega) - a^2\left(m^2 + 4i\omega + 1\right)\right]\mathcal{C}_{-,1}^{\infty} \\
&+ \frac{i}{6}\left\{a^3 m\left(m^2 + 12i\omega + 5\right) - 2a^2\left[3m^2(4\omega - i) + 4\omega(7 + 12i\omega)\right]\right. \\
&\left.+8am\left(24\omega^2 - 12i\omega - 1\right) + 64\omega\left(1 + 6i\omega - 8\omega^2\right)\right\}.
\end{aligned} \tag{C11f}$$

The initial values of $Y^{\mathrm{in}}(r)$ and $Y^{\mathrm{in}\prime}(r)$ at large $r = r_{\mathrm{out}}$ can then be obtained by integrating Eq. (38). The Y_+^{in} piece is straightforward and is given by

$$Y_+^{\mathrm{in}\prime}(r_{\mathrm{out}}) = -B_{\mathrm{SN}}^{\mathrm{ref}}\sum_{j=0}^{\infty}\frac{Y_{+,j}^{\infty}}{j+2}\frac{1}{r_{\mathrm{out}}^{j+2}}, \tag{C12a}$$

$$Y_+^{\rm in}(r_{\rm out}) = B_{\rm SN}^{\rm ref}\sum_{j=0}^{\infty}\frac{Y_{+,j}^{\infty}}{(j+1)(j+2)}\frac{1}{r_{\rm out}^{j+1}}. \tag{C12b}$$

While the $Y_-^{\rm in}$ piece is more complicated because the phase term is nonvanishing. We define

$$\begin{aligned} y_j(r_{\rm out}) \equiv& \int_{r_{\rm out}}^{\infty}\frac{e^{-2i\omega r}}{r^{j+4i\omega}} \\ =& \frac{1}{r_{\rm out}^{j-1+4i\omega}}\left[\frac{{}_1F_2\left(\frac{1-j}{2}-2i\omega;\frac{1}{2},\frac{3-j}{2}-2i\omega;-\omega^2r_{\rm out}^2\right)}{j-1+4i\omega}\right. \\ &\left.+\frac{2i\omega r_{\rm out}\times {}_1F_2\left(1-\frac{j}{2}-2i\omega;\frac{3}{2},2-\frac{j}{2}-2i\omega;-\omega^2r_{\rm out}^2\right)}{j-2+4i\omega}\right] \\ &+\frac{\Gamma(1-j-4i\omega)|2\omega|^{j+4i\omega}}{2}\left[\frac{1}{|\omega|}\sin\frac{\pi(j+4i\omega)}{2}-\frac{i}{\omega}\cos\frac{\pi(j+4i\omega)}{2}\right], \end{aligned} \tag{C13}$$

where ${}_1F_2(a;b,c;x)$ is the hypergeometric function. With these, we can write

$$Y_-^{\rm in\prime}(r_{\rm out}) = -\,e^{4i\omega\ln 2}B_{\rm SN}^{\rm inc}\sum_{j=0}^{\infty}Y_{-,j}^{\infty}y_{j+3}(r_{\rm out}), \tag{C14a}$$

$$\begin{aligned} Y_-^{\rm in}(r_{\rm out}) =& e^{4i\omega\ln 2}B_{\rm SN}^{\rm inc}\sum_{j=0}^{\infty}Y_{-,j}^{\infty}\left[y_{j+2}(r_{\rm out})\right. \\ &\left.-r_{\rm out}\cdot y_{j+3}(r_{\rm out})\right]. \end{aligned} \tag{C14b}$$

Unfortunately, using the hypergeometric function implemented in `HypergeometricFunctions.jl` [45] is too time-consuming for an acceptable precision when $\omega r_{\rm out}$ is a relatively large value. Therefore, we switch to an asymptotic expansion given by

$$\begin{aligned} &\frac{\Gamma(a_1)}{\Gamma(b_1)\Gamma(b_2)}{}_1F_2(a_1;b_1,b_2;-z) \\ &\quad= {}_1H_2(z) + {}_1E_2(ze^{-\pi i}) + {}_1E_2(ze^{\pi i}), \end{aligned} \tag{C15}$$

where

$${}_1H_2(z) = \sum_{j=0}^{\infty}\frac{(-1)^j}{j!}\frac{\Gamma(a_1+j)}{\Gamma(b_1-a_1-j)\Gamma(b_2-a_1-j)}z^{-a_1-j}, \tag{C16a}$$

$$\begin{aligned} {}_1E_2(z) =& \frac{e^{2\sqrt{z}}}{\sqrt{\pi}}\sum_{j=0}^{\infty}c_k\frac{z^{(\nu-j)/2}}{2^{j+1}} \\ =& \begin{cases} \frac{(-z)^{\nu/2}e^{-2i\sqrt{-z}}}{\sqrt{\pi}}\sum_{j=0}^{\infty}\frac{c_k(-z)^{-j/2}}{2^{j+1}} & z\to ze^{-\pi i} \\ \frac{(-z)^{\nu/2}e^{2i\sqrt{-z}}}{\sqrt{\pi}}\sum_{j=0}^{\infty}\frac{c_k(-z)^{-j/2}}{2^{j+1}} & z\to ze^{\pi i} \end{cases}, \end{aligned} \tag{C16b}$$

with

$$\nu = a_1 - b_1 - b_2 + \frac{1}{2}, \tag{C17a}$$

$$c_0 = 1, \tag{C17b}$$

$$c_j = -\frac{1}{4j}\sum_{w=0}^{j-1}c_w e_{j,w}, \tag{C17c}$$

$$\begin{aligned} e_{j,w} =& \frac{(1-\nu-2b_1+w)_{2+j-w}(a_1-b_1)}{(b_2-b_1)(1-b_1)} \\ &+\frac{(1-\nu-2b_2+w)_{2+j-w}(a_1-b_2)}{(b_1-b_2)(1-b_2)} \\ &+\frac{(w-1-\nu)_{2+j-w}(a_1-1)}{(1-b_1)(1-b_2)}. \end{aligned} \tag{C17d}$$

In our case, we have $b_2 = a_1 + 1$. Therefore,

$$\frac{\Gamma(a_1)}{\Gamma(b_1)\Gamma(b_2)} = \frac{1}{a_1\Gamma(b_1)}. \tag{C18}$$

Now we can construct the initial conditions for the ODE in Eq. (39) for $Y^{\rm in}$ and solve it inward to the horizon to get the values of $Y^{\rm in}$ and $Y^{\rm in\prime}$ across the entire domain of definition with

$$Y|_{r_*=r_*^{\rm out}} = Y_+^{\rm in}(r_{\rm out}) + Y_-^{\rm in}(r_{\rm out}), \tag{C19a}$$

$$\left.\frac{dY}{dr_*}\right|_{r_*=r_*^{\rm out}} = \frac{\Delta}{r_{\rm out}^2+a^2}\left[Y_+^{\rm in\prime}(r_{\rm out}) + Y_-^{\rm in\prime}(r_{\rm out})\right]. \tag{C19b}$$

Fig. 9 shows the relative error between the asymptotic expansion of $Y^{\rm in\prime\prime}(r\to\infty)$ defined in Eq. (38) and its definition in Eq. (30) by expanding up to $\sim\mathcal{O}(1/r^6)$ order. We can see that for larger values of ω, the asymptotic expansion converges rapidly to the definition. However, for smaller values of ω, the convergence decreases, and we need to have a larger $r_*^{\rm out}$, or equivalently, increase the expansion order. From our calculations, we find that generally setting $r_*^{\rm out} = \max(1000, 10\pi/|\omega|)$ is sufficient to reach the 10^{-12} relative tolerance if we truncate the expansion at $\sim\mathcal{O}(1/r^6)$ order.

2. The $Y^{\rm up}$ solution

Recall that in Ref. [13], we derived the asymptotic expansion of $X^{\rm up}$ for $r\to r_+$ as

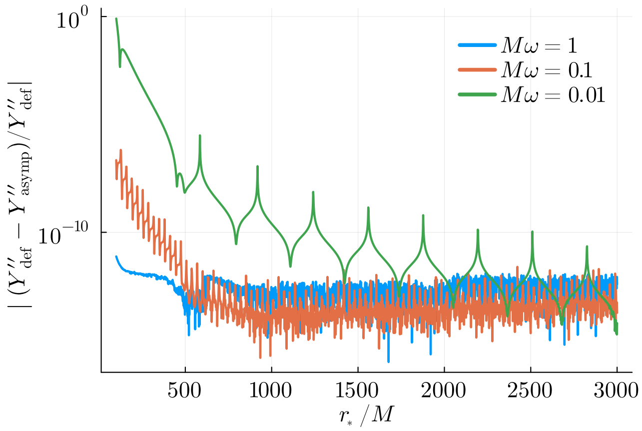

FIG. 9. The residue of the asymptotic expansion in Eq. (38) compared with the definition in Eq. (30) with $\ell = m = 2$, $a/M = 0.9$ and frequencies $M\omega = 1,\ 0.1,\ 0.01$. The asymptotic function is expanded to $\mathcal{O}(1/r^6)$ order.

$$X^{\rm up}(r \to r_+) = C_{\rm SN}^{\rm inc} e^{i\kappa r_*} \sum_{w=0}^{\infty} \mathcal{C}^{\rm H}_{+,w} (r - r_+)^w + C_{\rm SN}^{\rm ref} e^{-i\kappa r_*} \sum_{w=0}^{\infty} \mathcal{C}^{\rm H}_{-,w} (r - r_+)^w . \tag{C20}$$

Following the same procedure in Appendix C 1, we obtain

$$Y_+^{\rm up\prime\prime}(r \to r_+) = C_{\rm SN}^{\rm inc} \sum_{j=0}^{\infty} Y^{\rm H}_{+,j} (r - r_+)^j , \tag{C21a}$$

$$Y_-^{\rm up\prime\prime}(r \to r_+) = C_{\rm SN}^{\rm ref} \sum_{j=0}^{\infty} Y^{\rm H}_{-,j} (r - r_+)^{j+iq} , \tag{C21b}$$

where

$$q = \frac{(ar_+ m + 2a^2\omega - 4r_+\omega)}{r_+\sqrt{1-a^2}}. \tag{C22}$$

Unfortunately, the expressions of $Y^{\rm H}_{\pm,0,1,2}$ and $\mathcal{C}^{\rm H}_{\pm,0,1,2}$ are too long to show directly here and are available in a Mathematica notebook [44]. By combining Eq. (C21a) and Eq. (C21b), we obtain Eq. (40).

We then integrate Eqs. (C21) to get the initial values as

$$Y_+^{\rm up\prime}(r_{\rm in}) = C_{\rm SN}^{\rm inc} \sum_{j=0}^{\infty} Y^{\rm H}_{+,j} \frac{(r_{\rm in} - r_+)^{j+1}}{j+1}, \tag{C23a}$$

$$Y_+^{\rm up}(r_{\rm in}) = C_{\rm SN}^{\rm inc} \sum_{j=0}^{\infty} Y^{\rm H}_{+,j} \frac{(r_{\rm in} - r_+)^{j+2}}{(j+1)(j+2)}, \tag{C23b}$$

$$Y_-^{\rm up\prime}(r_{\rm in}) = C_{\rm SN}^{\rm ref} \sum_{j=0}^{\infty} Y^{\rm H}_{-,j} \frac{(r_{\rm in} - r_+)^{j+1+iq}}{j+1+iq}, \tag{C23c}$$

$$Y_-^{\rm up}(r_{\rm in}) = C_{\rm SN}^{\rm ref} \sum_{j=0}^{\infty} Y^{\rm H}_{-,j} \frac{(r_{\rm in} - r_+)^{j+2+iq}}{(j+1+iq)(j+2+iq)}. \tag{C23d}$$

Now we can also construct the initial conditions for the ODE in Eq. (39) for $Y^{\rm up}$ and solve it outward to infinity to get the initial values of $Y^{\rm up}(r)$ and $Y^{\rm up\prime}(r)$ across the entire domain of definition using

$$Y^{\rm up}\big|_{r_* = r_*^{\rm in}} = Y_+^{\rm up}(r_{\rm in}) + Y_-^{\rm up}(r_{\rm in}), \tag{C24a}$$

$$\left.\frac{dY^{\rm up}}{dr_*}\right|_{r_* = r_*^{\rm in}} = \frac{\Delta}{r_{\rm in}^2 + a^2}\left[Y_+^{\rm up\prime}(r_{\rm in}) + Y_-^{\rm up\prime}(r_{\rm in})\right]. \tag{C24b}$$

Appendix D: The expressions in $\mathcal{W}$ integrals

$$f_0(r) = \frac{\mathscr{A}}{\omega^2} w^{(0)}_{nn}(r) \sim \mathcal{O}(u^r), \tag{D1a}$$

$$f_1(r) = \frac{\mathscr{A}}{\omega^2}\left[w^{(0)\prime}_{nn}(r) + i\xi(r) w^{(0)}_{nn}(r) + w^{(1)}_{nn}(r)\right] \sim \mathcal{O}\left(\frac{u^r}{r}\right), \tag{D1b}$$

$$f_2(r) = \frac{\mathscr{A}}{\omega^2}\left[w^{(1)\prime}_{nn}(r) + i\xi(r) w^{(1)}_{nn}(r)\right] \sim \mathcal{O}\left(\frac{u^r}{r^2}\right), \tag{D1c}$$

$$g_0(r) = -\frac{\mathscr{A}}{i\omega} w^{(0)}_{n\bar{m}}(r) \sim \mathcal{O}(1), \tag{D1d}$$

$$g_1(r) = -\frac{\mathscr{A}}{i\omega}\left[w^{(0)\prime}_{n\bar{m}}(r) + i\xi(r) w^{(0)}_{n\bar{m}}(r) - w^{(1)}_{n\bar{m}}(r) + w^{(2)}_{n\bar{m}}(r)\right] \sim \mathcal{O}\left(\frac{1}{r}\right), \tag{D1e}$$

$$g_2(r) = \frac{\mathscr{A}}{i\omega}\left[\left(w^{(1)}_{n\bar{m}}(r) - w^{(2)}_{n\bar{m}}(r)\right)' + i\xi(r)\left(w^{(1)}_{n\bar{m}}(r) - w^{(2)}_{n\bar{m}}(r)\right)\right] \sim \mathcal{O}\left(\frac{1}{r^2}\right), \tag{D1f}$$

$$h_0(r) = -\mathscr{A}\frac{Sr^2\bar{\rho}^4\bar{\mathcal{M}}^2}{2\rho^2 u^r} \sim \mathcal{O}\left(\frac{1}{u^r}\right), \tag{D1g}$$

$$h_1(r) = -\mathscr{A}\left[\left(\frac{r^2}{\rho}\right)' + \frac{\left(r^2\rho^3\right)'}{\rho^4}\right]\frac{S\bar{\rho}^4\bar{\mathcal{M}}^2}{2\rho u^r} \sim \mathcal{O}\left(\frac{1}{ru^r}\right), \tag{D1h}$$

$$h_2(r) = -\mathscr{A}\left[\frac{\left(r^2\rho^3\right)'}{\rho^4}\right]'\frac{S\bar{\rho}^4\bar{\mathcal{M}}^2}{2\rho u^r} \sim \mathcal{O}\left(\frac{1}{r^2u^r}\right), \tag{D1i}$$

with

$$w_{nn}^{(0)}(r) = \frac{1}{2}r^2\rho\bar{\rho}^2u^r\mathscr{L}_1^\dagger\left[\rho^{-4}\mathscr{L}_2^\dagger\left(\rho^3S\right)\right], \tag{D2a}$$

$$w_{nn}^{(1)}(r) = w_{nn}^{(0)}(r)\left(\frac{\mathcal{N}}{u^r}\right)'\frac{u^r}{\mathcal{N}} + w_{nn}^{(0)\prime}(r) + i\xi(r)w_{nn}^{(0)}(r), \tag{D2b}$$

$$w_{n\bar{m}}^{(0)}(r) = \frac{r^2\bar{\rho}^3}{\rho}\bar{\mathcal{M}}\left[\mathscr{L}_2^\dagger S + ia\left(\rho-\bar{\rho}\right)\sin\theta S\right], \tag{D2c}$$

$$w_{n\bar{m}}^{(1)}(r) = \frac{r^2\bar{\rho}\bar{\mathcal{M}}}{2}\mathscr{L}_2^\dagger\left[\rho^3S\left(\bar{\rho}^2\rho^{-4}\right)'\right], \tag{D2d}$$

$$w_{n\bar{m}}^{(2)}(r) = \bar{\rho}\bar{\mathcal{M}}\left\{\frac{r^2\bar{\rho}^2}{\rho}\left[\mathscr{L}_2^\dagger S + ia\left(\rho-\bar{\rho}\right)\sin\theta S\right]\right\}'. \tag{D2e}$$

Appendix E: Solving for geodesic motions for Kerr black holes

The motion of a particle in a Kerr background is determined by the four constants of motion, namely the mass μ, energy E, angular momentum along the spin axis L_z, and Carter constant Q. In test mass limit, i.e., $\mu \ll 1$, the motion can be described by the following equations of motion in Kerr spacetime:

$$\Sigma\frac{dt}{d\tau} = -a\left(a\mathcal{E}\sin^2\theta - \mathcal{L}_z\right) + \frac{r^2+a^2}{\Delta}P, \tag{E1a}$$

$$\Sigma\frac{dr}{d\tau} = \pm\sqrt{R}, \tag{E1b}$$

$$\Sigma\frac{d\theta}{d\tau} = \pm\sqrt{\Theta}, \tag{E1c}$$

$$\Sigma\frac{d\varphi}{d\tau} = -\left(a\mathcal{E} - \frac{\mathcal{L}_z}{\sin^2\theta}\right) + \frac{a}{\Delta}P, \tag{E1d}$$

where

$$P = \mathcal{E}(r^2+a^2) - a\mathcal{L}_z, \tag{E2a}$$

$$R = P^2 - \Delta\left[r^2 + \left(\mathcal{L}_z - a\mathcal{E}\right)^2 + \mathcal{Q}\right], \tag{E2b}$$

$$\Theta = \mathcal{Q} - \cos^2\theta\left[a^2\left(1-\mathcal{E}^2\right) + \frac{\mathcal{L}_z^2}{\sin^2\theta}\right]. \tag{E2c}$$

Here the constants are rescaled by $\mathcal{E} \equiv E/\mu$, $\mathcal{L}_z \equiv L_z/\left(M\mu\right)$, and $\mathcal{Q} \equiv Q/\left(M\mu\right)^2$.

We follow the procedure in Ref. [46] to solve the equations. Here we outline the algorithm:

1. For a given set of orbital parameters, namely the spin parameter a, semi-letus rectum p, eccentricity e, and inclination parameter $x \equiv \cos\theta_{\rm inc}$, we follow Ref. [47] to map them to the constants of motion $(\mathcal{E},\ \mathcal{L}_z,\ \mathcal{Q})$.

2. Then we calculate the main frequencies of the motions by integrating the geodesic equations. By using the Mino time λ where $d\lambda \equiv d\tau/\Sigma$, we can decouple the r- and θ-direction motions [48] and obtain the Mino frequencies Υ_r and Υ_θ using elliptic integrals. We calculate the t- and φ-direction Mino frequencies Γ and Υ_φ, respectively, based on the r and θ motions.

3. Finally, we solve the geodesic equations by integrating them over one period, analytically expressing them as elliptic integrals using the Mino time λ, and extending them to full domain from $-\infty$ to ∞.

Following the above three steps, we obtain the solution of a generic timelike bound geodesic motion which can be written as Eqs. (63).

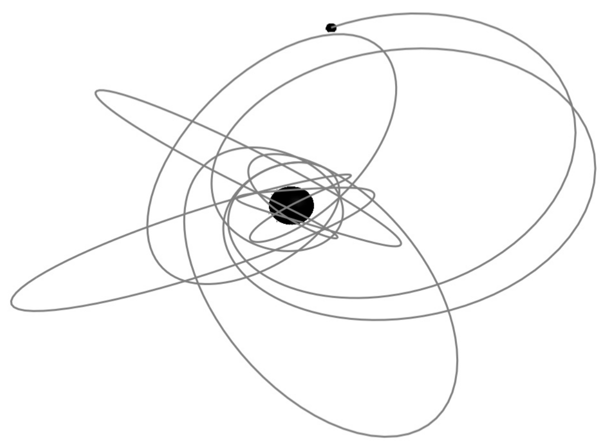

FIG. 10. A timelike bound geodesic trajectory around a Kerr black hole.

We implemented `KerrGeodesics.jl`[12], utilizing the high performance of `julia` to numerically compute the elliptic integrals (using the package `Elliptic.jl`). One

[12] https://github.com/CuberYyc808/KerrGeodesics.jl

can obtain all the ingredients for calculating the solution in microseconds. Fig. 10 shows the trajectory with $a = 0.9M$, $p = 6M$, $e = 0.7$, $x = \cos\pi/4$, which corresponds to the waveform in Fig. 3.

Currently, unbound geodesics are not available in the package. We plan to include plunge orbits (see Ref. [49]) and scattering orbits (see Ref. [50]) in the future.

Appendix F: Levin's method

The evaluation of highly oscillatory integrals, such as Eq. (66) when n and k are large, is difficult and often encountered in a wide range of problems. To tackle this issue, we employ Levin's method [51], which converts the quadrature problem into an equivalent system of ODEs that gives the anti-derivative function of the integrand kernel. In the following, we briefly illustrate Levin's method for one-dimensional integrals.

For a one-dimensional integral of the form

$$\mathbb{I} = \int_a^b f(r) e^{ig(r)} dr, \tag{F1}$$

where the phase function $g(r)$ varies rapidly while the kernel function $f(r)$ varies slowly, we want to find the solution of $p(r)$ that satisfies the following ODE

$$p'(r) + ig'(r)p(r) = f(r). \tag{F2}$$

With $p(r)$, $\mathbb{I}$ can be evaluated using simply

$$\mathbb{I} = p(b)e^{ig(b)} - p(a)e^{ig(a)}. \tag{F3}$$

Following Ref. [52], we solve Eq. (F2) for $p(r)$ using a Chebyshev spectral method. The ODE problem is further transformed into a problem of solving a system of linear equations given by

$$\left[\overleftrightarrow{D} + i\,\overleftrightarrow{g'}\right]\,\vec{p} = \vec{f}, \tag{F4}$$

where $\overleftrightarrow{D}$ is the differentiation matrix, $\overleftrightarrow{g'}$ and $\vec{f}$ are a diagonal matrix and a vector evaluated at the collocation points, respectively. We refer readers to a detailed exposition of the algorithm for one-dimensional integrals and the two-dimensional generalization in Refs. [52] and [53], respectively.

To facilitate the calculations in this work, we implemented an optimized version of the adaptive Levin's algorithm following Refs. [52, 53] in `julia`, which is publicly available as `AdaptiveLevin.jl`[13].

[13] https://github.com/CuberYyc808/AdaptiveLevin.jl

[1] B. P. Abbott *et al.* (LIGO Scientific, Virgo), Observation of Gravitational Waves from a Binary Black Hole Merger, Phys. Rev. Lett. **116**, 061102 (2016), arXiv:1602.03837 [gr-qc].

[2] A. G. Abac *et al.* (LIGO Scientific, VIRGO, KAGRA), GWTC-4.0: Population Properties of Merging Compact Binaries (2025), arXiv:2508.18083 [astro-ph.HE].

[3] A. G. Abac *et al.* (LIGO Scientific, Virgo, KAGRA), GW250114: Testing Hawking's Area Law and the Kerr Nature of Black Holes, Phys. Rev. Lett. **135**, 111403 (2025), arXiv:2509.08054 [gr-qc].

[4] J. Aasi *et al.* (LIGO Scientific), Advanced LIGO, Class. Quant. Grav. **32**, 074001 (2015), arXiv:1411.4547 [gr-qc].

[5] F. Acernese *et al.* (VIRGO), Advanced Virgo: a second-generation interferometric gravitational wave detector, Class. Quant. Grav. **32**, 024001 (2015), arXiv:1408.3978 [gr-qc].

[6] K. Somiya (KAGRA), Detector configuration of KAGRA: The Japanese cryogenic gravitational-wave detector, Class. Quant. Grav. **29**, 124007 (2012), arXiv:1111.7185 [gr-qc].

[7] M. Colpi *et al.*, LISA Definition Study Report (2024), arXiv:2402.07571 [astro-ph.CO].

[8] P. Amaro-Seoane, Relativistic dynamics and extreme mass ratio inspirals, Living Reviews in Relativity **21**, 4 (2018), arXiv:1205.5240 [astro-ph.CO].

[9] S. Babak, J. Gair, A. Sesana, E. Barausse, C. F. Sopuerta, C. P. L. Berry, E. Berti, P. Amaro-Seoane, A. Petiteau, and A. Klein, Science with the space-based interferometer LISA. V: Extreme mass-ratio inspirals, Phys. Rev. D **95**, 103012 (2017), arXiv:1703.09722 [gr-qc].

[10] C. P. L. Berry, S. A. Hughes, C. F. Sopuerta, A. J. K. Chua, A. Heffernan, K. Holley-Bockelmann, D. P. Mihaylov, M. C. Miller, and A. Sesana, The unique potential of extreme mass-ratio inspirals for gravitational-wave astronomy, Bull. Am. Astron. Soc. **51**, 42 (2019), arXiv:1903.03686 [astro-ph.HE].

[11] S. Chandrasekhar, *The mathematical theory of black holes* (1985).

[12] S. A. Teukolsky, Perturbations of a rotating black hole. 1. Fundamental equations for gravitational electromagnetic and neutrino field perturbations, Astrophys. J. **185**, 635 (1973).

[13] R. K. L. Lo, Recipes for computing radiation from a Kerr black hole using a generalized Sasaki-Nakamura formalism: Homogeneous solutions, Phys. Rev. D **110**, 124070 (2024), arXiv:2306.16469 [gr-qc].

[14] S. Mano, H. Suzuki, and E. Takasugi, Analytic solutions of the Teukolsky equation and their low frequency expansions, Prog. Theor. Phys. **95**, 1079 (1996), arXiv:gr-qc/9603020.

[15] R. Fujita and H. Tagoshi, New Numerical Methods to Evaluate Homogeneous Solutions of the Teukolsky Equation, Progress of Theoretical Physics **112**, 415 (2004), https://academic.oup.com/ptp/article-pdf/112/3/415/5382220/112-3-415.pdf.

[16] R. Fujita and H. Tagoshi, New Numerical Methods to Evaluate Homogeneous Solutions of the Teukolsky

Equation. II: — Solutions of the Continued Fraction Equation —, Progress of Theoretical Physics **113**, 1165 (2005), https://academic.oup.com/ptp/article-pdf/113/6/1165/5285582/113-6-1165.pdf.

[17] M. Sasaki and T. Nakamura, A class of new perturbation equations for the kerr geometry, Physics Letters A **89**, 68 (1982).

[18] M. Sasaki and T. Nakamura, Gravitational Radiation from a Kerr Black Hole. I. Formulation and a Method for Numerical Analysis, Progress of Theoretical Physics **67**, 1788 (1982), https://academic.oup.com/ptp/article-pdf/67/6/1788/5332324/67-6-1788.pdf.

[19] Y. Jiang and W.-B. Han, A New High-Performing Method for Solving the Homogeneous Teukolsky Equation (2025), arXiv:2507.15363 [gr-qc].

[20] S. Drasco and S. A. Hughes, Gravitational wave snapshots of generic extreme mass ratio inspirals, Phys. Rev. D **73**, 024027 (2006), [Erratum: Phys.Rev.D 88, 109905 (2013), Erratum: Phys.Rev.D 90, 109905 (2014)], arXiv:gr-qc/0509101.

[21] E. Poisson, Gravitational radiation from infall into a black hole: Regularization of the Teukolsky equation, Phys. Rev. D **55**, 639 (1997), arXiv:gr-qc/9606078.

[22] M. Sasaki and H. Tagoshi, Analytic Black Hole Perturbation Approach to Gravitational Radiation, Living Reviews in Relativity **6**, 6 (2003), arXiv:gr-qc/0306120 [gr-qc].

[23] D. Watarai, Ringdown of a postinnermost stable circular orbit of a rapidly spinning black hole: Mass ratio dependence of higher harmonic quasinormal mode excitation, Phys. Rev. D **110**, 124029 (2024), arXiv:2408.16747 [gr-qc].

[24] T. Nakamura, K. Oohara, and Y. Kojima, General relativistic collapse to black holes and gravitational waves from black holes, Progress of Theoretical Physics Supplement **90**, 1 (1987), https://academic.oup.com/ptps/article-pdf/doi/10.1143/PTPS.90.1/5201911/90-1.pdf.

[25] M. Shibata, Gravitational waves induced by a particle orbiting around a rotating black hole: Effect of orbital precession, Progress of Theoretical Physics **90**, 595 (1993), https://academic.oup.com/ptp/article-pdf/90/3/595/5161685/90-3-595.pdf.

[26] N. Sago and T. Tanaka, Gravitational wave echoes induced by a point mass plunging into a black hole, Progress of Theoretical and Experimental Physics **2020**, 123E01 (2020).

[27] K. Glampedakis and D. Kennefick, Zoom and whirl: Eccentric equatorial orbits around spinning black holes and their evolution under gravitational radiation reaction, Phys. Rev. D **66**, 044002 (2002).

[28] S. A. Hughes, Evolution of circular, nonequatorial orbits of kerr black holes due to gravitational-wave emission, Phys. Rev. D **61**, 084004 (2000).

[29] M. Shibata, Gravitational waves induced by a particle orbiting around a rotating black hole: Spin-orbit interaction effect, Phys. Rev. D **48**, 663 (1993).

[30] M. Shibata, Gravitational waves by compact star orbiting around rotating supermassive black holes, Phys. Rev. D **50**, 6297 (1994).

[31] Black Hole Perturbation Toolkit, (bhptoolkit.org).

[32] Z. Nasipak, Adiabatic evolution due to the conservative scalar self-force during orbital resonances, Phys. Rev. D **106**, 064042 (2022).

[33] Z. Nasipak, Adiabatic gravitational waveform model for compact objects undergoing quasicircular inspirals into rotating massive black holes, Phys. Rev. D **109**, 044020 (2024).

[34] E. Mitsou, Gravitational radiation from radial infall of a particle into a schwarzschild black hole: A numerical study of the spectra, quasinormal modes, and power-law tails, Phys. Rev. D **83**, 044039 (2011).

[35] L. Smarr, Gravitational radiation from distant encounters and from head-on collisions of black holes: The zero-frequency limit, Phys. Rev. D **15**, 2069 (1977).

[36] E. Berti, V. Cardoso, T. Hinderer, M. Lemos, F. Pretorius, U. Sperhake, and N. Yunes, Semianalytical estimates of scattering thresholds and gravitational radiation in ultrarelativistic black hole encounters, Phys. Rev. D **81**, 104048 (2010).

[37] V. Cardoso and J. P. S. Lemos, Gravitational radiation from the radial infall of highly relativistic point particles into Kerr black holes, Phys. Rev. D **67**, 084005 (2003), arXiv:gr-qc/0211094.

[38] A. J. K. Chua, M. L. Katz, N. Warburton, and S. A. Hughes, Rapid generation of fully relativistic extreme-mass-ratio-inspiral waveform templates for LISA data analysis, Phys. Rev. Lett. **126**, 051102 (2021), arXiv:2008.06071 [gr-qc].

[39] M. L. Katz, A. J. K. Chua, L. Speri, N. Warburton, and S. A. Hughes, Fast extreme-mass-ratio-inspiral waveforms: New tools for millihertz gravitational-wave data analysis, Phys. Rev. D **104**, 064047 (2021), arXiv:2104.04582 [gr-qc].

[40] L. Speri, M. L. Katz, A. J. K. Chua, S. A. Hughes, N. Warburton, J. E. Thompson, C. E. A. Chapman-Bird, and J. R. Gair, Fast and Fourier: Extreme Mass Ratio Inspiral Waveforms in the Frequency Domain, Front. Appl. Math. Stat. **9**, 10.3389/fams.2023.1266739 (2024), arXiv:2307.12585 [gr-qc].

[41] C. E. A. Chapman-Bird *et al.*, The Fast and the Frame-Dragging: Efficient waveforms for asymmetric-mass eccentric equatorial inspirals into rapidly-spinning black holes (2025), arXiv:2506.09470 [gr-qc].

[42] Z. Zhang, E. Berti, and V. Cardoso, Quasinormal ringing of Kerr black holes. II. Excitation by particles falling radially with arbitrary energy, Phys. Rev. D **88**, 044018 (2013), arXiv:1305.4306 [gr-qc].

[43] R. K. L. Lo, L. Sabani, and V. Cardoso, Quasinormal modes and excitation factors of Kerr black holes, Phys. Rev. D **111**, 124002 (2025), arXiv:2504.00084 [gr-qc].

[44] Y. Yin, R. K. L. Lo, and X. Chen, 10.5281/zenodo.17574059.

[45] R. M. Slevinsky and other contributors, `HypergeometricFunctions.jl`, `https://github.com/JuliaMath/HypergeometricFunctions.jl` (2018-2025).

[46] R. Fujita and W. Hikida, Analytical solutions of bound timelike geodesic orbits in Kerr spacetime, Class. Quant. Grav. **26**, 135002 (2009), arXiv:0906.1420 [gr-qc].

[47] W. Schmidt, Celestial mechanics in kerr spacetime, Classical and Quantum Gravity **19**, 2743 (2002).

[48] Y. Mino, Perturbative approach to an orbital evolution around a supermassive black hole, Phys. Rev. D **67**, 084027 (2003), arXiv:gr-qc/0302075.

[49] C. Dyson and M. van de Meent, Kerr-fully diving into the abyss: analytic solutions to plunging geodesics in Kerr, Class. Quant. Grav. **40**, 195026 (2023), arXiv:2302.03704 [gr-qc].

[50] D. Bini, A. Geralico, and J. Vines, Hyperbolic scattering of spinning particles by a kerr black hole, Phys. Rev. D **96**, 084044 (2017).
[51] D. Levin, Procedures for computing one- and two-dimensional integrals of functions with rapid irregular oscillations, Mathematics of Computation **38**, 531 (1982).
[52] S. Chen, K. Serkh, and J. Bremer, On the adaptive levin method, Numer. Math. **156**, 1927–1985 (2024).
[53] S. Chen, K. Serkh, J. Bremer, and M. Aubry, An adaptive delaminating Levin method in two dimensions (2025), arXiv:2506.02424 [cs.NA].